

# A *Plasmodium falciparum* MORC protein complex modulates epigenetic control of gene expression through interaction with heterochromatin

Maneesh Kumar Singh<sup>1†</sup>, Victoria Ann Bonnell<sup>2,3,4†</sup>, Israel Tojal Da Silva<sup>5</sup>, Verônica Feijoli Santiago<sup>6</sup>, Miriam Santos Moraes<sup>1</sup>, Jack Adderley<sup>7</sup>, Christian Doerig<sup>7</sup>, Giuseppe Palmisano<sup>6</sup>, Manuel Llinas<sup>2,3,4,8</sup>, Celia RS Garcia<sup>1\*</sup>

<sup>1</sup>Department of Clinical and Toxicological Analyses, School of Pharmaceutical Sciences, University of São Paulo, São Paulo, Brazil; <sup>2</sup>Department of Biochemistry and Molecular Biology, Pennsylvania State University, University Park, Harrisburg, United States; <sup>3</sup>Huck Institutes Center for Eukaryotic Gene Regulation, Pennsylvania State University, University Park, Harrisburg, United States; <sup>4</sup>Huck Institutes Center for Malaria Research, Pennsylvania State University, University Park, Harrisburg, United States; <sup>5</sup>Hospital AC Camargo, Centro Internacional de Pesquisa, São Paulo, Brazil; <sup>6</sup>Department of Parasitology, Institute of Biomedical Science, University of São Paulo, São Paulo, Brazil; <sup>7</sup>School of Health and Biomedical Sciences, RMIT University, Bundoora, Australia; <sup>8</sup>Department of Chemistry, Pennsylvania State University, University Park, Harrisburg, United States

\*For correspondence: [cgarcia@usp.br](mailto:cgarcia@usp.br)

†These authors contributed equally to this work

**Competing interest:** The authors declare that no competing interests exist.

**Funding:** See page 16

**Preprint posted**  
11 September 2023

**Sent for Review**  
18 September 2023

**Reviewed preprint posted**  
16 November 2023

**Reviewed preprint revised**  
01 May 2024

**Version of Record published**  
16 October 2024

**Reviewing Editor:** Sebastian Lourido, Whitehead Institute for Biomedical Research, United States

© Copyright Singh, Bonnell et al. This article is distributed under the terms of the [Creative Commons Attribution License](https://creativecommons.org/licenses/by/4.0/), which permits unrestricted use and redistribution provided that the original author and source are credited.

**Abstract** Dynamic control of gene expression is critical for blood stage development of malaria parasites. Here, we used multi-omic analyses to investigate transcriptional regulation by the chromatin-associated microorchidia protein, MORC, during asexual blood stage development of the human malaria parasite *Plasmodium falciparum*. We show that *Pf*MORC (PF3D7\_1468100) interacts with a suite of nuclear proteins, including APETALA2 (ApiAP2) transcription factors (*Pf*AP2-G5, *Pf*AP2-O5, *Pf*AP2-I, PF3D7\_0420300, PF3D7\_0613800, PF3D7\_1107800, and PF3D7\_1239200), a DNA helicase DS60 (PF3D7\_1227100), and other chromatin remodelers (*Pf*CHD1 and *Pf*EELM2). Transcriptomic analysis of *Pf*MORC<sup>HA-glmS</sup> knockdown parasites revealed 163 differentially expressed genes belonging to hypervariable multigene families, along with upregulation of genes mostly involved in host cell invasion. In vivo genome-wide chromatin occupancy analysis during both trophozoite and schizont stages of development demonstrates that *Pf*MORC is recruited to repressed, multigene families, including the *var* genes in subtelomeric chromosomal regions. Collectively, we find that *Pf*MORC is found in chromatin complexes that play a role in the epigenetic control of asexual blood stage transcriptional regulation and chromatin organization.

## eLife assessment

This study provides **valuable** insights into how chromatin-bound *Pf*MORC controls gene expression in the asexual blood stage of *Plasmodium falciparum*. By interacting with key nuclear proteins, *Pf*MORC is predicted to affect expression of genes relating to host invasion and variable subtelomeric gene families. Correlating transcriptomic data with in vivo chromatin analysis, the study provides **convincing** evidence for the role of *Pf*MORC in epigenetic transcriptional regulation.

## Introduction

Despite global efforts to combat malaria, the disease caused an estimated 249 million new cases and more than 608,000 deaths in 2022 (World Malaria Report 2023). The etiological agents of human malaria are apicomplexan parasites of the genus *Plasmodium*. Among the six known *Plasmodium* species that can infect humans, *Plasmodium falciparum* is the most lethal, causing the majority of annual deaths (Cowman et al., 2012). The intraerythrocytic developmental cycle (IDC) of *P. falciparum* is responsible for the clinical symptoms of malaria. The IDC commences when merozoites generated during the liver stage enter the circulatory system and invade red blood cells (RBCs). While growing inside RBCs, parasites undergo multiple developmental phases with distinct morphological characteristics (ring, trophozoite, and schizont). Maturation and schizogony lead to the formation of 16–32 daughter merozoites destined to invade new RBCs (Singh et al., 2010). A small fraction (<10%) of parasites differentiate into non-replicative sexual gametocytes, which are transmitted to the mosquito during a second blood meal to complete sexual development.

Parasite development through the asexual blood stage is facilitated by precise transcriptional regulation, where genes are only expressed when needed in a just-in-time fashion (Bozdech et al., 2003). Approximately 90% of genes across the *P. falciparum* genome are transcribed during the asexual blood stage in a cascade of gene expression believed to be controlled by both sequence-specific transcription factors and dynamic epigenetic changes to chromatin (Painter et al., 2011; Toenhake et al., 2018; Jeninga et al., 2019; Hollin et al., 2021). The gene regulatory toolbox in malaria parasites is lacking many transcriptional regulatory factors conserved in other eukaryotes (Gardner et al., 2002). The identification of a large family of *Plasmodium* homologs of the plant APETALA2/Ethylene Response Factor (AP2/ERF) transcription factors (TFs) provided a breakthrough to unravel key regulators of gene expression in these parasites (Balaji et al., 2005). There are 28 putative APETALA2 (ApiAP2) TFs identified in *P. falciparum*, each protein containing 1–3 AP2 DNA binding domains (Painter et al., 2011; Jeninga et al., 2019). Multiple studies in *Plasmodium* spp., using a variety of approaches, have characterized essential functions of ApiAP2 TFs in RBC invasion, gametocytogenesis, oocyst formation, and sporozoite formation (Yuda et al., 2009; Kafsack et al., 2014; Sinha et al., 2014; Modrzynska et al., 2017; Santos et al., 2017; Zhang et al., 2018). ApiAP2 proteins in *Plasmodium* species display a wide array of functions during parasite development in both the vertebrate host and the mosquito vector, but surprisingly, over 70% of ApiAP2 proteins are expressed in the asexual blood stage of the lifecycle (Bozdech et al., 2003; Le Roch et al., 2003; Chappell et al., 2020).

Despite increasing evidence detailing ApiAP2 protein regulatory complexes (Santos et al., 2017; Harris et al., 2019; Hillier et al., 2019; Hoeijmakers et al., 2019; Farhat et al., 2020; Josling et al., 2020; Miao et al., 2021; Srivastava et al., 2023; Yuda et al., 2023; Antunes et al., 2024), the functional properties and specific interaction partners of many ApiAP2 TFs remain to be elucidated. A quantitative mass spectrometry-based analysis of the parasite protein interaction network has revealed links between ApiAP2 TFs and many chromatin remodelers, such as an extended Egl-27 and MTA1 homology 2 (EELM2) domain-containing proteins (PF3D7\_0519800 and PF3D7\_1141800), histone deacetylase protein 1 (HDAC1; PF3D7\_0925700), and the microorchidia family protein PfmMORC (PF3D7\_1468100) (Hillier et al., 2019). Genome-wide mutagenesis studies revealed that several genes within these proposed networks, including *pfmorc*, are essential for parasite proliferation (Bushell et al., 2017; Zhang et al., 2018). Using a targeted deletion strategy, we previously were unable to delete *pfmorc*, further suggesting that it is essential for parasite growth (Singh et al., 2021a). Moreover, STRING network analysis has shown that the putative ApiAP2:PfmMORC complex forms a network with proteins having DNA-binding or nucleosome assembly properties, suggesting that PfmMORC may function as an accessory protein in epigenetic regulation (Hillier et al., 2019). Previous work identified PfmMORC in a chromatin complex containing the chromatin remodeling protein PflSWI (PF3D7\_0624600) located at *var* gene promoter regions (Bryant et al., 2020). All *P. falciparum* strains encode roughly 60 highly polymorphic *var* genes, but through an epigenetic allelic exclusion mechanism, each parasite is thought to express a single allele (Real et al., 2022; Schneider et al., 2023). Bryant et al. have proposed that PfmMORC is recruited to these heterochromatic regions to assist in the silencing of *var* genes, on the basis of its known function as a repressor complex component in model eukaryotes. In the related apicomplexan parasite *Toxoplasma gondii*, TgMORC functions as a repressor of sex-associated genes by recruiting the TgHDAC3 histone deacetylase and forming

heterogenous complexes with 11 ApiAP2 TFs (Farhat et al., 2020). To date, only two TgMORC:HDAC3 complexes have been characterized, including a dimeric TgAP2XII-2:HDAC3 complex and a heterotrimeric TgAP2XII-1:AP2XII-2:HDAC3 complex (Srivastava et al., 2023; Antunes et al., 2024).

MORC proteins canonically consist of two major conserved regions: (1) a catalytic ATPase domain at the N-terminus (comprising a GHKL [Gyrase, HSP90, Histidine kinase, and MutL] domain and S5 fold domain) and (2) a C-terminal protein-protein interaction domain containing one or more coiled-coils (Koch et al., 2017). The conserved MORC gene family is present in most eukaryotes (with the exception of fungi), often with multiple paralogs per genome (Dong et al., 2018), and has been extensively investigated in various model systems in the context of epigenetic gene regulation. In plants, MORC proteins function in gene repression and heterochromatin compaction (Koch et al., 2017; Zhong et al., 2023). Additionally, MORC proteins have been shown to play diverse roles in metazoans by forming protein-protein interactions with immune-responsive proteins, SWI chromatin remodeling complexes, histone deacetylases, and histone tail modifications (Iyer et al., 2008b, Kang et al., 2012; Moissiard et al., 2012; Bordiya et al., 2016; Kim et al., 2019).

While most metazoans possess 5–7 MORC paralogs, apicomplexan parasites contain a single *morc* gene (Iyer et al., 2008a), which encodes not only the canonical animal-like GHKL ATPase domain, but also three Kelch-repeats, and a CW-type zinc-finger domain not found in mammalian MORCs (Farhat et al., 2020). This unique domain architecture suggests that the apicomplexan MORC proteins may have parasite-specific roles. To dissect the functional roles of *PfMORC*, we conducted a proteomic analysis with *PfMORC*<sup>GFP</sup>, which identified several nuclear proteins, including a cluster of ApiAP2 TFs, as possible interacting partners. We also determined the genome-wide localization of *PfMORC* at multiple developmental stages, which revealed *PfMORC* recruitment predominantly to subtelomeric regions, corroborating that *PfMORC* may act as a repressor of the clonally variant gene families that are important contributors to malaria pathogenesis. Finally, we performed transcriptomic analysis in *PfMORC*<sup>HA-glmS</sup> knockdown parasites at the asexual stage to investigate alterations in global gene expression. We observed an overrepresentation of downregulated genes belonging to the heterochromatin-associated hypervariable gene family proteins. Overall, this study allows us to assign a role for *PfMORC* in facilitating the plasticity of epigenetic regulation during asexual blood stage development.

## Results

### Proteins that co-purify with PMORC represent gene regulatory and chromatin remodeling components

A previous study using Blue-Native PAGE identified a *PfMORC* complex in association with ApiAP2 proteins and chromatin remodeling machinery (Hillier et al., 2019). To validate this observation and expand the repertoire of *PfMORC* interactors, we used a targeted immunoprecipitation approach coupled to LC-MS/MS proteomic quantification. We used a previously generated *PfMORC*<sup>GFP</sup> parasite line (Singh et al., 2021a) to carry out immunoprecipitation with an anti-GFP antibody at the trophozoite stage, where *PfMORC* is abundant (Singh et al., 2021b). The *P. falciparum* 3D7 strain expressing wild-type *pfmorc* was used as a negative control. Trophozoite lysates were incubated with anti-GFP-Trap-A beads (ChromoTek, gta-20), and the immunocaptured proteins were resolved by SDS-PAGE (Figure 1—figure supplement 1A). We applied a label-free quantitative proteomics approach with a false discovery rate (FDR) of 1% and number of peptides  $\geq 2$  to excised gel samples to identify proteins interacting with *PfMORC*<sup>GFP</sup>. From three biological replicates, we identified 211, 617, and 656 proteins, respectively. We further identified the overlap between all three wild-type 3D7 and *PfMORC*<sup>GFP</sup> replicates and found a total of 132 and 142 proteins, respectively (Figure 1—figure supplement 1B–D, Supplementary file 1).

To analyze the relative ratio of proteins between wild-type 3D7 and *PfMORC*<sup>GFP</sup> groups, we used the mean-normalized MS/MS count to calculate a fold change from *PfMORC*<sup>GFP</sup>/3D7, and selected differentially abundant proteins above a 1.5 $\times$  cutoff filter. This high stringency threshold was used to preclude any mis-identification of *PfMORC* interactors caused by variability between the replicates (Figure 1A, Figure 1—figure supplement 1D). This analysis resulted in 143 significantly enriched proteins (Supplementary file 2). From these candidate *PfMORC*-interacting proteins, the top enriched protein (20.8-fold enrichment) was *PfEELM2* (PF3D7\_0519800,  $-\log_{10}$  p-value 3.43). *PfEELM2*

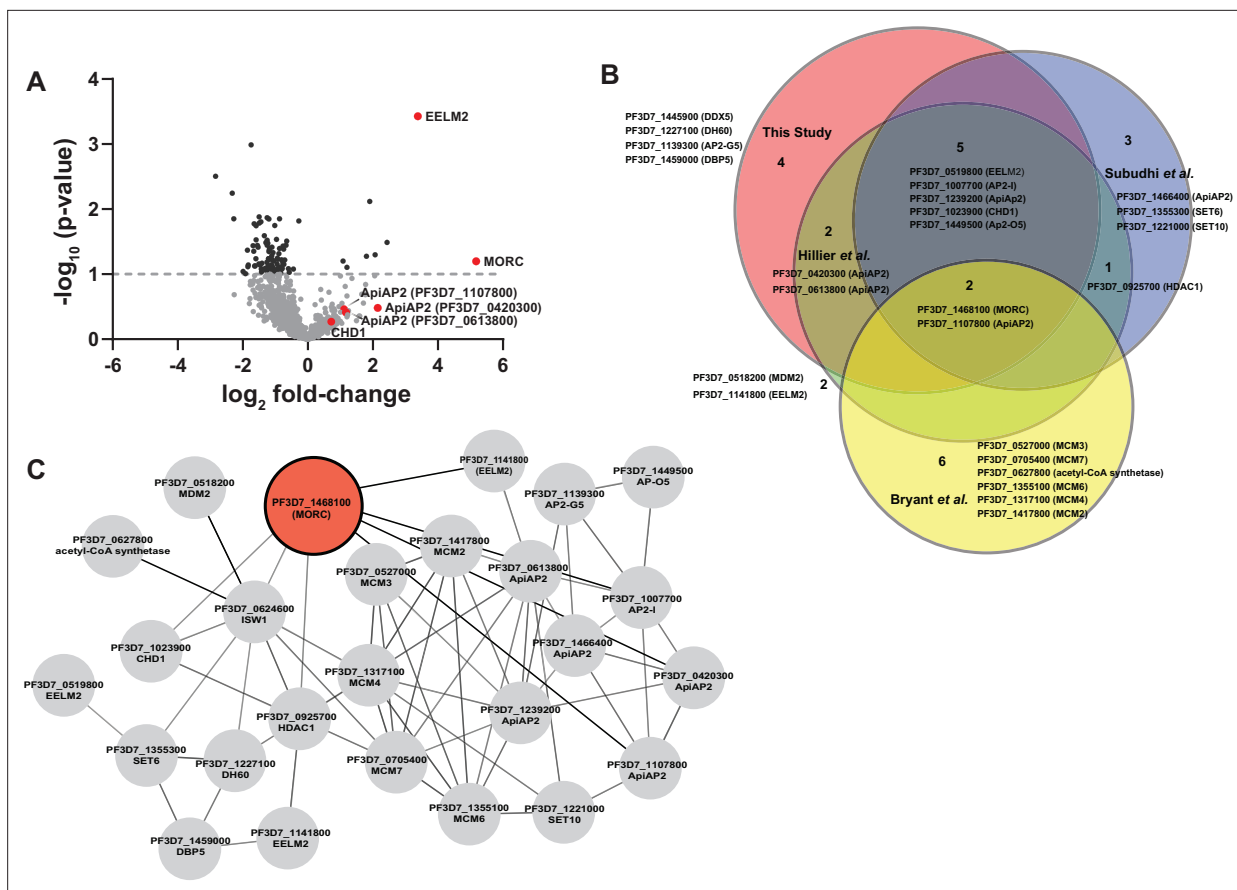


**Figure 1.** Proteomic analysis of parasites expressing *PfMORC*<sup>GFP</sup> reveals *PfMORC* association with nuclear proteins of epigenetic regulation. **(A)** Volcano plot illustrates the protein enrichment in label free LC-MS/MS analysis of *PfMORC* ColPed proteins from three independent experiments at 32 hours post invasion (hpi). For normalized MS/MS counts, Student's *t*-test was performed and proteins were ranked as  $-\log_{10}$  fold-change (x-axis) versus statistical *p*-values (y-axis). Gray dashed horizontal line shows the *p*-value cutoff. **(B)** Comparative analysis showing the juxtaposition of specific proteins ColPed in *PfMORC*<sup>GFP</sup> with selected proteins from recent works of Hillier et al., Bryant et al., and Subudhi et al., where ApiAP2 or ISW1 were used as bait in similar ColP experiments. The Venn diagram illustrates the overlap between identified proteins, revealing that the intersecting proteins are primarily ApiAP2 and chromatin remodellers. **(C)** An interactive protein–protein interaction network is constructed with proteins known to interact with *PfMORC*, using proteins identified in this study and proteins documented in previously published works. Proteins identified in this study with known interaction networks from the STRING database were used to curate the network employing Cytoscape to enrich the network quality.

The online version of this article includes the following source data and figure supplement(s) for figure 1:

**Figure supplement 1.** Proteomic analysis of *PfMORC* interacting proteins identified in *Plasmodium falciparum* lysate.

**Figure supplement 1—source data 1.** Uncropped and labeled SDSPAGE gel.

**Figure supplement 1—source data 2.** Raw unedited SDSPAGE gel.

was previously predicted as a *PfMORC* interactor (Hillier et al., 2019) and identified in a quantitative histone peptide pull-down to be consistently recruited to H2B.Z\_K13/14/18a (Hoeijmakers et al., 2019). Similarly, EELM2 of the related Apicomplexan parasite *T. gondii* was recently identified in a *TgMORC*-associated complex (Farhat et al., 2020). We also detected numerous ApiAP2 transcription factors (*PfAP2*-G5, *PfAP2*-O5, *PfAP2*-I, PF3D7\_1107800, PF3D7\_0613800, PF3D7\_0420300, and PF3D7\_1239200) (Table 1), similar to results reported both by Hillier et al., 2019 and in the *Toxoplasma* studies which also predicted or experimentally identified many ApiAP2 interactions (Farhat et al., 2020; Srivastava et al., 2023; Antunes et al., 2024). *PfAP2*-G5 (PF3D7\_1139300,  $-\log_{10}$  *p*-value 0.22) and *PfAP2*-O5 (PF3D7\_1449500,  $-\log_{10}$  *p*-value 0.41) were enriched 20.5-fold and 14.99-fold, respectively, suggesting that these factors are likely major components in complex with *PfMORC*. To corroborate our results, we compared our *PfMORC*<sup>GFP</sup> colPed proteins to a recently published, computationally predicted, protein–protein interaction network (Hillier et al., 2019; Bryant et al., 2020; Subudhi et al., 2023) and found many of ApiAP2 and EELM2 proteins shared across both

**Table 1.** Potential *PfMORC* interacting proteins enriched in CoIP eluates and identified in LC-MS/MS from three independent experiments and fold change  $\geq 1.5\times$  GFP/3D7.

Protein ID	Annotation	Fold change	-log p-value	Known function
PF3D7_0519800	EELM2 domain-containing protein	20.79	3.45	-
PF3D7_1139300	AP2 domain transcription factor AP2-G5	20.5	0.22	Repressor of commitment and early gametocyte development ( <i>Shang et al., 2021a</i> )
PF3D7_1449500	AP2 domain transcription factor AP2-O5	14.99	0.41	Regulator of mature ookinete motility ( <i>Modrzynska et al., 2017</i> )
PF3D7_1468100	<i>PfMORC</i>	11.76	1.20	
PF3D7_1023900	SNF2 helicase, putative or Chromodomain-helicase-DNA-binding protein 1 homolog, CHD1	10.61	0.30	
PF3D7_1459000	ATP-dependent RNA helicase DBP5	10.24	0.46	
PF3D7_1227100	DNA helicase 60, DH60	6.55	0.41	-
PF3D7_1007700	AP2 domain transcription factor AP2-I	4.65	0.08	Invasion ( <i>Santos et al., 2017; Josling et al., 2020</i> )
PF3D7_1107800	AP2 domain transcription factor	3.11	0.36	Master regulator of parasite growth, chromatin structure, and <i>var</i> gene expression ( <i>Subudhi et al., 2023</i> )
PF3D7_0613800	AP2 domain transcription factor	2.43	0.28	-
PF3D7_0420300	AP2 domain transcription factor (ApiAP2)	2.38	0.48	-
PF3D7_0624600	SNF2 helicase, ISW1	2.09	0.001	<i>var</i> gene expression ( <i>Bryant et al., 2020</i> )
PF3D7_1239200	AP2 domain transcription factor	2.01	0.25	-

datasets (**Figure 1B**). Collectively, our results demonstrate a direct association of *PfMORC* with various chromatin-associated factors, including at least seven ApiAP2 proteins.

The potential interactors of *PfMORC* that we detected in this experiment also included proteins implicated in DNA replication and repair, including the ATP-dependent RNA helicase DBP5 (PF3D7\_1459000,  $-\log_{10}$  p-value 0.46) and the DNA helicase 60 DH60 (PF3D7\_1227100,  $-\log_{10}$  p-value 0.41). *PfDH60* exhibits DNA and RNA unwinding activities, and its high expression in the trophozoites suggests a role in DNA replication (*Pradhan et al., 2005*). We also identified two putative chromatin-associated proteins, chromodomain-helicase-DNA-binding protein 1 CHD1 (PF3D7\_1023900,  $-\log_{10}$  p-value 0.30) and the SNF2 chromatin-remodeling ATPase ISWI (PF3D7\_0624600,  $-\log_{10}$  p-value 0.001), which are associated with chromosome structure maintenance, DNA replication, DNA repair, and transcription regulation. *PfISWI* was previously reported to be associated with *PfMORC* in the context of *var* gene transcriptional activation during ring stage development (*Bryant et al., 2020*). Gene Ontology (GO) analysis was performed to identify enriched biological processes, cellular components, and molecular functions using a p-value cutoff of 0.05. We found significant enrichment of DNA-binding transcription factor activity and mRNA binding, transcription, and regulation of transcription activity (**Figure 1—figure supplement 1E, Supplementary file 3**). Overall, we again find that *PfMORC* forms a link between ApiAP2 TFs and chromatin remodelers (**Figure 1C**).

### ***PfMORC* localizes to multigene families in subtelomeric regions**

To determine the genome-wide occupancy of the *PfMORC* chromatin-associated remodeling complex, we used chromatin immunoprecipitation followed by high-throughput sequencing (ChIP-seq). Using purified, crosslinked nuclear extracts, we immunoprecipitated *PfMORC* from a 3xHA-tagged *PfMORC*<sup>HA-gImS</sup> parasite line (*Singh et al., 2021a*) for ChIP-seq at the trophozoite stage (30 hpi) and the schizont stage (40 hpi) in biological duplicates. These timepoints represent the stages at which *PfMORC* expression is the highest (*Singh et al., 2021b*). An independent ChIP-seq experiment in biological duplicate using anti-GFP and a *PfMORC*<sup>GFP</sup> parasite line (*Singh et al., 2021b*) at the schizont stage was used to confirm our findings, demonstrating that the protein tags do not affect *PfMORC* immunoprecipitation or genome-wide localization (**Figure 2—figure supplement 1A and B**). As an additional control, we correlated one no-epitope (3D7 wild type), negative control sample using the same anti-HA antibody on unmodified parasite lines for immunoprecipitation (**Figure 2—figure**



**supplement 1A and B; Bonnell et al., 2023**), which resulted in an expected low correlation to the tagged samples. The biological ChIP-seq replicates showed high fold enrichment ( $\text{Log}_2[\text{IP}/\text{Input}]$ ) (**Figure 2—figure supplement 1C**) and were highly correlated with each other within each timepoint (**Figure 2—figure supplement 1D–F**).

We identified *PfMORC* localized to subtelomeric regions on all chromosomes across the *P. falciparum* genome, with additional occupancy at internal heterochromatic islands (**Figure 2A and B**). Within the subtelomeric regions, *PfMORC* was bound upstream and within the gene bodies of many hypervariable multigene families (**Figure 2C**), including *var* genes (**Figure 2—figure supplement 2**), *rif* genes (**Figure 2—figure supplement 3**), and *stevor* genes (**Figure 2—figure supplement 4**). Predicted binding sites (across both biological replicates) between the 30 hpi and 40 hpi time-points showed a high degree of overlap, suggesting that *PfMORC* binds many of the same regions throughout the later stages of asexual development when *PfMORC* is highly expressed (**Figure 2D**). The proportion of *PfMORC*-bound regions was similar across the 5' upstream region of genes and the gene bodies throughout the genome, including subtelomeric regions (**Figure 2E**). As opposed to the binding of other proteins at the subtelomeric regions, such as the heterochromatin protein 1 (*PfHP1*) (**Flueck et al., 2010**), *PfMORC* occupancy is not widespread. Instead, it forms sharp peaks within, and adjacent to, HP1-bound regions (**Figure 2F**), suggesting a unique role for *PfMORC* in heterochromatin condensation, boundary demarcation, and gene repression.

We further defined *PfMORC* putative gene targets as genes displaying peaks within 2 kb upstream of the ATG start codon or within gene bodies. For those peaks between gene targets in a head-to-head orientation, the closest gene was chosen. This resulted in 149 putative gene targets at 30 hpi and 102 gene targets at 40 hpi. A close examination of the 84 overlapping genes shows that many are *var* genes, rRNA genes, and genes encoding exported proteins (**Supplementary file 4**), with GO terms related to cell adhesion, host–pathogen interactions, and antigenic variation (**Supplementary file 5**). The 65 uniquely bound genes at the 30 hpi timepoint showed an enrichment of highly expressed tRNA and rRNAs genes, as well as conserved unknown genes, while those 18 unique to the 40 hpi timepoint included a variety of late-stage expressed genes. Transcript abundance (**Chappell et al., 2020**) of the predicted *PfMORC* gene targets at both the 30 hpi and 40 hpi timepoints form two major clusters: cluster 1 being genes expressed at the late ring/early trophozoite stage (10–24 hpi) and cluster 2 at the late schizont stage (40–48 hpi) (**Figure 2—figure supplement 5**). This two-cluster gene target pattern of expression mirrors the biphasic pattern of expression by *PfMORC*, suggesting that *PfMORC* could have distinct functions, forming complexes with different sets of transcriptional regulators, at various times during asexual proliferation. As determined in other eukaryotic organisms, MORC family proteins do not generally bind DNA in a sequence-specific manner; it is, therefore, likely that *PfMORC* is recruited to these genome-wide regions by sequence-specific transcription factors, such as the ApiAP2 proteins identified in our proteomics results.

## Binding sites of *PfMORC* overlap with ApiAP2 proteins and epigenetic marks

*PfMORC* has previously been found to interact with several ApiAP2 proteins (**Hillier et al., 2019; Bryant et al., 2020; Singh et al., 2021b**), as does the *Toxoplasma* ortholog (**Farhat et al., 2020; Srivastava et al., 2023; Antunes et al., 2024**). We identified a clear overlap between genome-wide *PfMORC* binding and putatively interacting ApiAP2 proteins using available ChIP-seq datasets. In addition to our protein–protein interaction results (**Table 1**), previous studies have also suggested that *PfMORC* interacts with a broad array of ApiAP2 TFs, such as *PfAP2-G5*, *PfAP2-O5*, *PfAP2-I*, PF3D7\_1107800, PF3D7\_0613800, PF3D7\_0420300, and PF3D7\_1239200 (**Hillier et al., 2019; Bryant et al., 2020; Subudhi et al., 2023**). Therefore, we compared binding sites between interacting ApiAP2s and *PfMORC* using available ChIP-seq data on *PfAP2-G5*, *PfAP2-O5*, *PfAP2-I*, PF3D7\_1107800, PF3D7\_0613800, and PF3D7\_1239200 (**Josling et al., 2020; Shang et al., 2021b, Shang et al., 2022**). Interestingly, there is a degree of overlap between the binding sites of all six ApiAP2 TFs and *PfMORC*, suggesting that *PfMORC* and these ApiAP2 TFs may cooperate in the regulation of gene expression at these loci (**Figure 3A and B, Figure 3—figure supplement 1**). However, the available data cannot differentiate whether all these factors are in one complex together, form multiple smaller heterologous complexes, or are components of separate complexes in individual cells. DNA motif enrichment analysis (**Bailey, 2021**) identified several unique and significant DNA

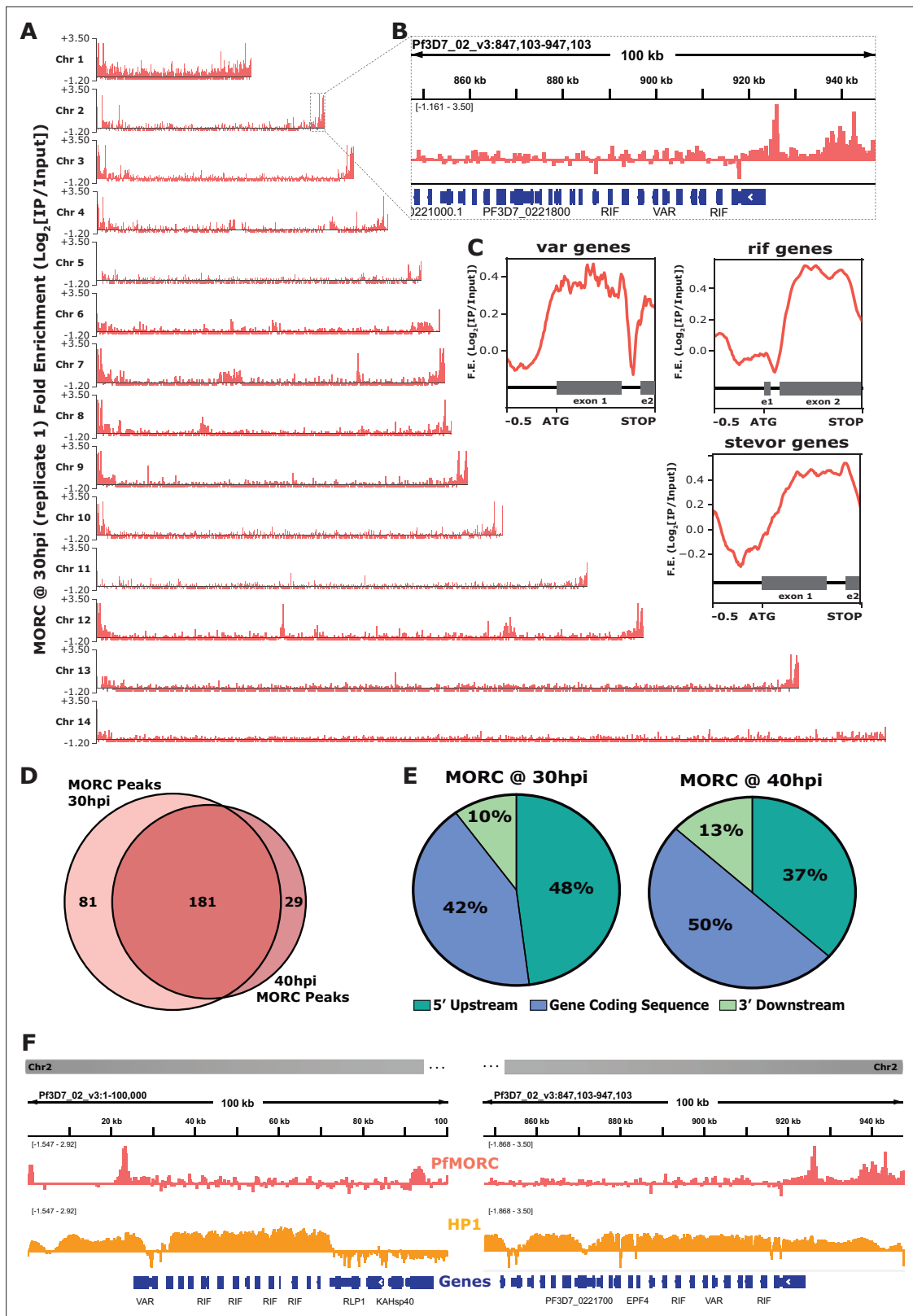


**Figure 2.** Genome-wide occupancy of *PfMORC* reveals localization to hypervariable surface antigen genes at 30 hr and 40 hr. **(A)** Coverage tracks of *PfMORC* across all 14 *P. falciparum* chromosomes. Plotted values are fold enrichment ( $\text{Log}_2[\text{IP}/\text{Input}]$ ) of a representative replicate at 30 hr. **(B)** Zoom-in of the last 100 kb region of chromosome two from **(A)**. Gene annotations represented in blue bars (*P. falciparum* 3D7 strain, version 3, release 57; [PlasmDB.org](https://plasmadb.org)). **(C)** Mean fold enrichment of *PfMORC* occupancy across all *var* genes (top left), all *rif* genes (top right), and all *stevor* genes (bottom). *Figure 2 continued on next page*

Figure 2 continued

right), excluding pseudogenes. Graphical representation of exons to scale for each gene family annotated below enrichment plot in grey (e1 = exon one; e2 = exon two). (D) Quantitative Venn diagram comparing the number of MACS2 called peaks across each timepoint (light pink for 30 hr; dark pink for 40 hr). (E) Pie charts showing the type of genomic locations *PfMORC* peaks overlap at both 30 hr and 40 hr. Pink slices are 5' regions upstream of the ATG start site of genes, blue slices are coding sequences/gene bodies of genes, and green slices are 3' regions downstream of the stop codon of genes. (F) Zoom-in of the first 100 kb region (left) and the last 100 kb region (right) of chromosome two. Plotted are the ChIP-seq fold enrichment of *PfMORC* (top track; pink) and heterochromatin protein 1 (HP1; middle track; orange) with gene annotations (bottom track; blue bars; *P. falciparum* 3D7 strain, version 3, release 57; [PlasmoDB.org](https://plasmodb.org)).

The online version of this article includes the following figure supplement(s) for figure 2:

**Figure supplement 1.** Comparison of ChIP-seq enriched peaks across different *PfMORC* samples.

**Figure supplement 2.** ChIP-seq profiling of *PfMORC* fold enrichment across var gene regions.

**Figure supplement 3.** ChIP-seq profiling of *PfMORC* fold enrichment across *rif* gene regions.

**Figure supplement 4.** ChIP-seq profiling of *PfMORC* fold enrichment across *stevor* gene regions.

**Figure supplement 5.** The heatmaps show the transcript abundance ([Chappell et al., 2020](#)) of putative *PfMORC* gene targets at 30 hr (A) and 40 hr (B).

motifs at both the 30 hpi and 40 hpi timepoints, which suggests that more than one sequence-specific transcription factor may be responsible for recruiting *PfMORC* to specific genomic regions (**Figure 3—figure supplement 2**). The common motifs identified across replicates and timepoints are RGTGCAW or TGCACACA, both of which are similar or identical to the *in vitro* and/or *in vivo* DNA-binding motif of *PfAP2-I* (RGTGCAW) or *PF3D7\_0420300* (TGCACACA), respectively, suggesting that these *ApiAP2* factors may play major roles in *PfMORC* recruitment (**Figure 3—figure supplement 2**).

In addition to overlapping occupancy with *ApiAP2* TFs, we found that *PfMORC* co-localizes with the depletion of H3K36me2 (**Figure 3C and D**), which is demarcated by the SET2 methyltransferase ([Jiang et al., 2013](#)), both at 30 hpi and 40h pi. No other significant co-localization was found between *PfMORC* and other epigenetic marks (H2A.Z, H3K9ac, H3K4me3, H3K27ac, H3K18ac, H3K9me3, H3K36me2/3, H4K20me3, and H3K4me1) (**Figure 3—figure supplement 3**), suggesting it has a unique binding preference not shared with other heterochromatin markers. Therefore, it is likely that *PfMORC* co-localizes with other, as yet uncharacterized, epigenetic marks. In summary, *PfMORC* was found to be recruited to 5'-untranslated regions (UTRs), gene body regions, and subtelomeric regions of repressed, multigene families, and overlaps with other known *ApiAP2* binding sites and DNA motifs.

## Depletion of *PfMORC* results in the upregulation of late-stage genes associated with invasion

*PfMORC* association with chromatin remodelers has been shown ([Bryant et al., 2020](#)), but how *PfMORC* regulates gene expression in the asexual stage has not been evaluated. In *T. gondii*, the TgMORC:TgApiAP2 complex acts as a transcriptional repressor of sexual commitment ([Farhat et al., 2020](#); [Srivastava et al., 2023](#); [Antunes et al., 2024](#)). Here, we found that *PfMORC* co-immunoprecipitates with several chromatin remodeling proteins and many *ApiAP2* transcription factors. Furthermore, our ChIP-seq data revealed that *PfMORC* is located at subtelomeric regions of the genome. Based on this evidence, we hypothesized that *PfMORC* may regulate transcriptional changes during blood stage development of the parasite. To knock down the expression of *PfMORC* (*PfMORC-KD*), sorbitol-synchronized MORC<sup>HA-glmS</sup> parasites (22–24 hpi) were subjected to 2.5 mM glucosamine (GlcN) treatment for little over 48 hr when they reached the trophozoite stage (32 hpi ±3 hpi), at which point parasites were harvested for RNA isolation for transcriptomic analysis. In parallel, another flask with *PfMORC*<sup>HA-glmS</sup> parasites was set up without GlcN and used as control for RNA-seq comparison. We previously demonstrated that treatment with 2.5 mM GlcN results in a 50% knockdown of *PfMORC* protein but does not cause any growth delay; using >2.5 mM GlcN caused a measurable slow growth and reduced parasitemia ([Singh et al., 2021b](#)). Three biological replicates with and without 2.5 mM GlcN were collected for knockdown transcriptomics to ensure reproducibility.

For each *PfMORC* RNA-seq sample, gene counts were used to identify the differentially expressed genes (DEGs). Significant threshold parameters were assigned to a p-value<0.05, yielding a total of 2558 DEGs (**Supplementary file 6**). Applying a log<sub>2</sub>-fold change cutoff from >1 to <-1 and filtering out pseudogenes reduced this number to 163 DEGs. Among these, 60 genes display more abundant transcripts, whereas 103 genes were reduced relative to control parasites grown without GlcN



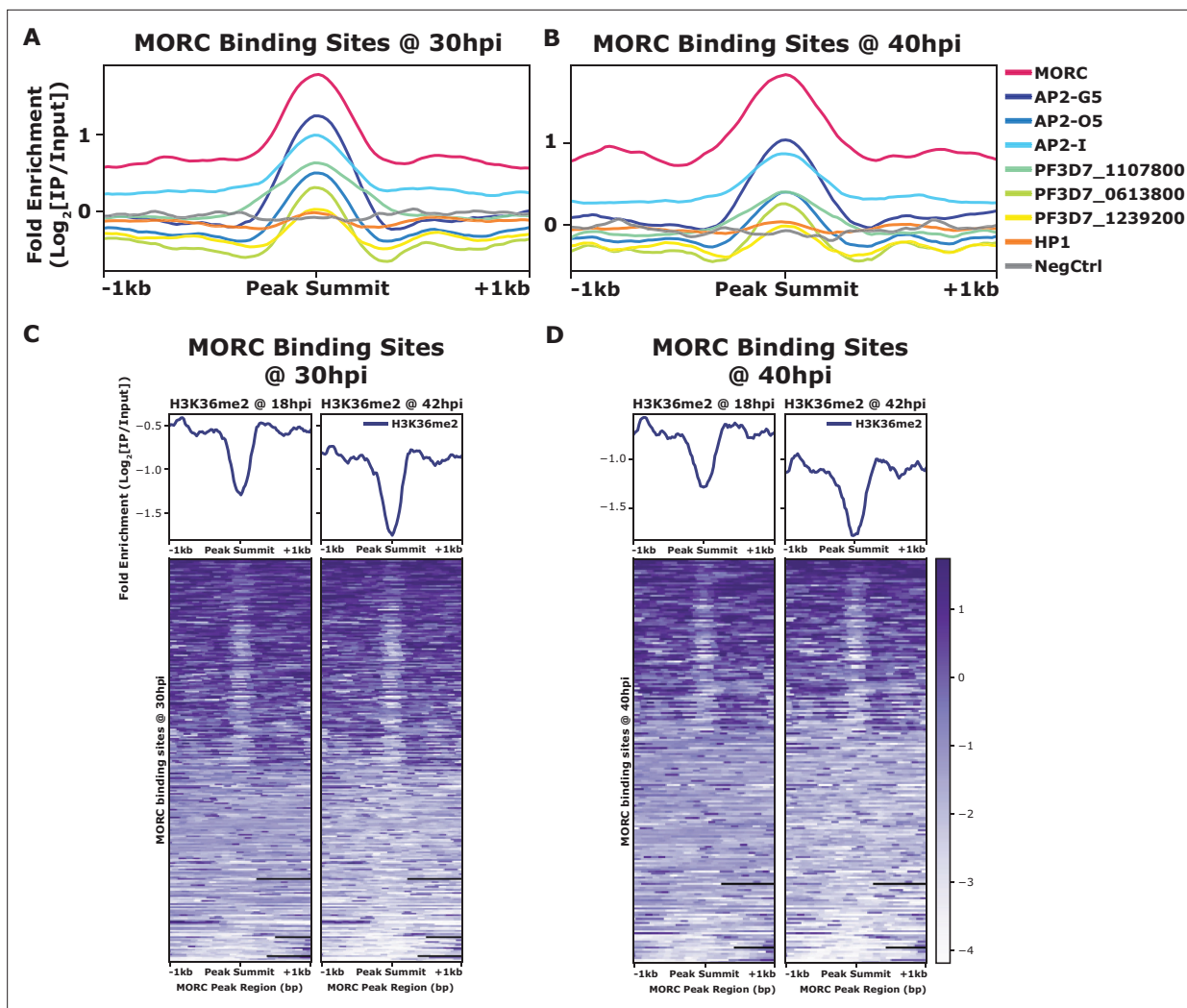


**Figure 3.** Comparison of mean fold enrichment of *PfMORC* with ApiAP2 transcription factors and other epigenetic markers at different time points. **(A)** Mean fold enrichment ( $\text{Log}_2[\text{IP}/\text{Input}]$ ) of *PfMORC*, six associated factors (AP2-G5, AP2-O5, AP2-I, PF3D7\_1107800, PF3D7\_0613800, and PF3D7\_1239200), HP1, and a negative no-epitope control across *PfMORC* binding sites at the 30 hr timepoint. **(B)** Mean fold enrichment ( $\text{Log}_2[\text{IP}/\text{Input}]$ ) of *PfMORC*, six associated factors (AP2-G5, AP2-O5, AP2-I, PF3D7\_1107800, PF3D7\_0613800, and PF3D7\_1239200), HP1, and a negative no-epitope control across *PfMORC* binding sites at the 40 hr timepoint. **(C)** Mean fold enrichment ( $\text{Log}_2[\text{IP}/\text{Input}]$ ) and heatmap of two H3K36me2 epigenetic mark timepoints across *PfMORC* binding sites at 30 hr. **(D)** Mean fold enrichment ( $\text{Log}_2[\text{IP}/\text{Input}]$ ) and heatmap of two H3K36me2 epigenetic mark timepoints across *PfMORC* binding sites at 40 hr.

The online version of this article includes the following figure supplement(s) for figure 3:

**Figure supplement 1.** Overlap between *PfMORC* and other ApiAP2 transcription factors binding regions.

**Figure supplement 2.** DNA motif analyses from these different categories: (1) unique to 30 hpi ChIP-seq timepoint, (2) 30 hpi ChIP-seq timepoint, (3) overlap of ChIP-seq timepoint, (4) 40 hpi ChIP-seq timepoint, and (5) unique to 40 hpi ChIP-seq timepoint.

**Figure supplement 3.** Mean fold enrichment ( $\text{Log}_2[\text{IP}/\text{Input}]$ ) summary plot (top) and full heatmap (bottom) of fold enrichment of 10 selected epigenetic marks (H2A.Z, H3K9ac, H3K4me3, H3K27ac, H3K18ac, H3K9me3, H3K36me2/3, H4K20me3, and H3K4me1) across *PfMORC* binding sites at the 30 hr and 40 hr timepoints.

(**Figure 4A**). Pathway and functional enrichment analysis yielded several genes from apical organelles. GO analysis revealed gene clusters enriched with molecular function ( $p\text{-adj}=0.0006$ ) involved in the movement into the host environment and entry into the host, and molecular function of protein binding ( $p\text{-adj}=0.009$ ) (**Figure 4B, Supplementary file 7**). More specifically, upregulated genes implicated in the invasion of merozoites were found to be expressed prematurely upon *PfMORC* KD; these include several rohyptry-associated genes, notably *PfRON2* (PF3D7\_1452000) and *PfRON3* (PF3D7\_1252100). Both *PfRON2* and *PfRON3* are part of a micronemal complex at the erythrocyte

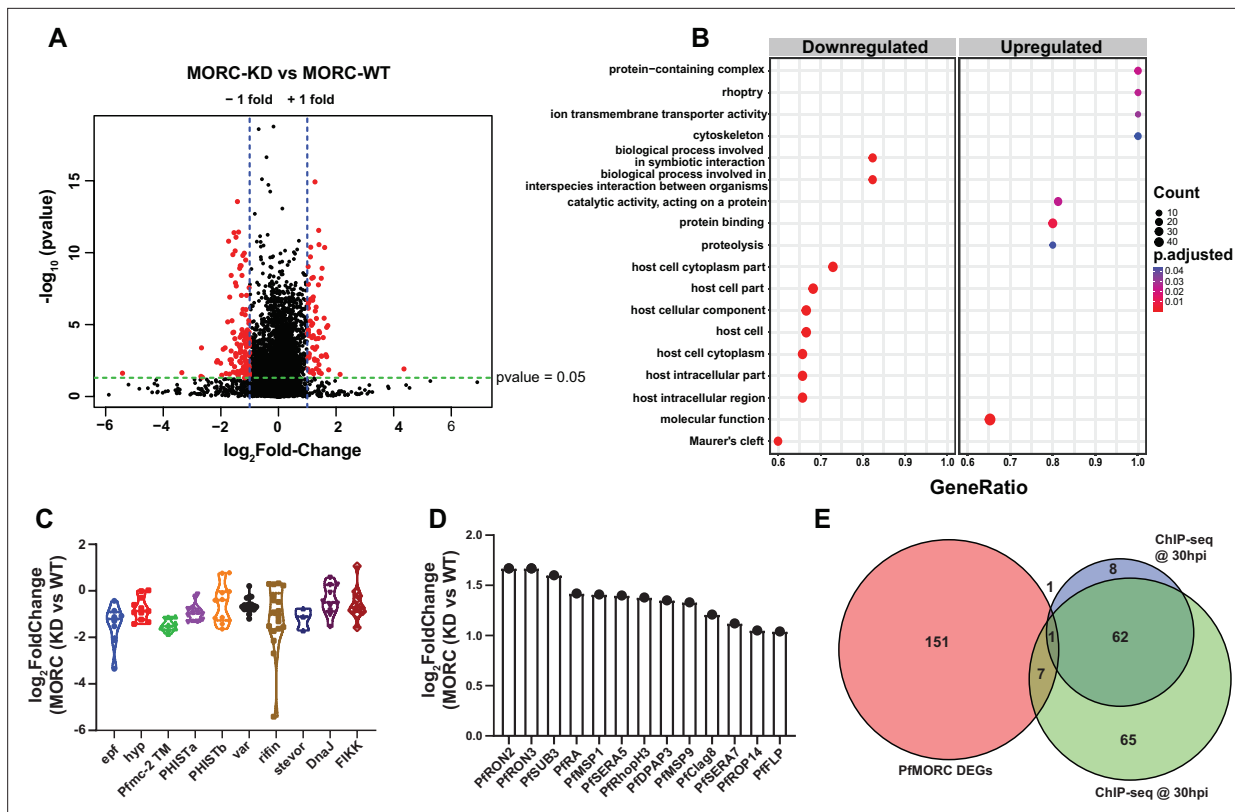


**Figure 4.** Transcriptome analysis of *PfMORC* knockdown revealed differential gene expression. **(A)** Volcano plot displaying the differential gene expression in *PfMORC*-KD compared to the *PfMORC*-WT phenotype. Tightly synchronized *PfMORC*<sup>HA-glmS</sup> parasites (32 hpi ± 3 hr) were split into two populations, one of which was treated with 2.5 mM GlcN to obtain the *PfMORC* knockdown phenotype and the other was not treated with GlcN to obtain wild-type phenotype. Total RNA-seq was performed, and significant threshold parameters for differentially expressed genes (DEGs) were assigned to a p-value <0.05 and -log<sub>2</sub> fold change >1 from three biological replicates. **(B)** Scatter plot shows upregulated and downregulated DEGs which were further categorized for pathway and functional enrichment analysis using the KEGG database (p-adjusted value <0.05). The circle size at the vertical axis represents the number of genes in the enriched pathways and the horizontal axis represents gene richness as a ratio of DEGs in the pathways to the total genes in a specific pathway. **(C)** The violin plot of log<sub>2</sub> fold change of genes belonging to the multigene family is constructed from *PfMORC*-KD vs. *PfMORC*-WT, which shows DEGs of multigene family proteins upon *PfMORC* knockdown. **(D)** The bar plot illustrates the upregulated DEGs of apical organelle origin in *PfMORC*-KD parasites involved in host cell invasion. **(E)** Venn diagram showing the comparison between genes obtained from ChIP-seq data and DEGs obtained from RNA-seq data. Both 30hpi and 40 hpi timepoints were taken for comparison and showed high overlap with each other but there was no overlap with RNA-seq data.

The online version of this article includes the following figure supplement(s) for figure 4:

**Figure supplement 1.** Comparison of transcriptional changes with melatonin treatment.

membrane where *PfRON2* anchors *PfAMA1* to facilitate merozoite invasion (Srinivasan et al., 2013). In addition, *PfSUB3* (PF3D7\_0507200), *PfSERA5* (PF3D7\_0207600), and *PfDPA3* (PF3D7\_0404700), all of which are critical for schizont rupture (Yeoh et al., 2007; Arastu-Kapur et al., 2008), were among the upregulated DEGs (Figure 4C). In general, we found that depletion of *PfMORC* leads to the upregulation of invasion-related genes, which suggests that *PfMORC* has an additional function in the regulation of genes specifically associated with RBC invasion.

### *PfMORC*-depleted parasites downregulate hypervariable gene families

Among the genes with reduced mRNA abundance, DEGs linked to cytoadherence, antigenic variation, and interaction with host (Figure 4B and D) were over-represented in the GO analysis. Many of the genes enriched in the downregulated group belong to the clonally variant *var* multigene family that represents 60 members encoding the *P. falciparum* erythrocyte membrane proteins (*PfEMP1*), which upon switching expression aid in pathogenesis and immune evasion (Guizetti and Scherf, 2013). Furthermore, a cluster of genes encoding putative exported proteins were also enriched

including members of the exported protein family (EPFs), *Plasmodium* exported protein (hyp), and *Plasmodium* exported protein (PHISTa/b). Other significantly overrepresented downregulated genes belonged to serine/threonine protein kinases, the FIKK family (Ward et al., 2004), most of which are exported to the RBC, and Maurer's clefts two transmembrane proteins (PfmC-2TM) (Figure 4D). Notably, expressed proteins are conserved across the *Plasmodium* family and remain confined to the hypervariable subtelomeric region of *P. falciparum* chromosomes (Sargeant et al., 2006).

## Comparison of ChIP-seq gene targets and DEGs by RNA-seq

To identify whether genes found to be dysregulated after PfMORC knockdown are associated with the genome-wide occupancy of PfMORC, we correlated the gene targets identified by ChIP-seq with the DEGs determined by RNA-seq. We identified a total of 135 gene targets from the 30 hpi ChIP-seq timepoint, 72 gene targets from the 40 hpi ChIP-seq timepoint, and 163 DEGs by RNA-seq. The low correlation between the ChIP-seq gene targets and the RNA-seq DEGs suggests that PfMORC genome-wide occupancy is more likely involved in chromatin structure, rather than specific regulation of gene targets (Figure 4E). Likely, PfMORC localizes to these sites to aid in chromatin condensation, as shown in other eukaryotic systems (Zhang et al., 2019; Zhong et al., 2023).

## Discussion

Periodic gene expression during the asexual blood stage directly corresponds to the timing in which gene products are needed (Bozdech et al., 2003) and shows oscillation patterns associated with circadian rhythms (Smith et al., 2020; Subudhi et al., 2020). Transcription factors are critical regulators of this dynamic pattern in concert with epigenetic regulators and genome-wide changes to chromatin structure (Painter et al., 2011; Toenhake et al., 2018; Jeninga et al., 2019; Hollin et al., 2021). The ApiAP2 family members display unique binding preferences in the genome (Campbell et al., 2010), undergo stage-specific expression (Painter et al., 2011), and have been identified to regulate virtually all stages of development across multiple *Plasmodium* species (Jeninga et al., 2019). To date, ApiAP2 proteins have been reported in transcriptional silencing of clonally variant genes, regulation of invasion genes, and sexual commitment, acting through interaction with other epigenetic factors, such as heterochromatin protein 1 [PfHP1 (Flueck et al., 2010; Brancucci et al., 2014; Fraschka et al., 2018)], bromodomain protein 1 [PfBDP1 (Santos et al., 2017; Josling et al., 2020; Quinn et al., 2022)], or general control non-depressible 5 [PfGCN5 (Miao et al., 2021)]. Despite the known DNA-binding sites of many ApiAP2 proteins (Flueck et al., 2010; Santos et al., 2017; Sierra-Miranda et al., 2017; Josling et al., 2020; Carrington et al., 2021; Shang et al., 2021b; Singh et al., 2021a, Russell et al., 2022; Shang et al., 2022; Bonnell et al., 2023), limited information is available for other accessory proteins. Recently, the *T. gondii* ortholog TgMORC was identified in a complex with HDAC1, AP2XII-2, and AP2XII-1:AP2XI-2 and orchestrates epigenetic rewiring of sexual gene transcription (Farhat et al., 2020; Srivastava et al., 2023; Antunes et al., 2024). In *P. falciparum*, PfMORC has been copurified with several ApiAP2 proteins, as shown by different independent studies (Hillier et al., 2019; Bryant et al., 2020; Singh et al., 2021b).

In this study, we used an integrated multi-omics approach to explore the function of PfMORC during asexual blood stage development. Using immunoaffinity-based purification, we identified a number of nuclear proteins that interact with PfMORC. More specifically, PfMORC was associated with PfAP2-G5, which is essential for gametocytogenesis (Shang et al., 2021b), PfAP2-I, which is required for the expression of many invasion-related genes (Santos et al., 2017), and with other ApiAP2 TFs of unknown function (PfAP2-O5, PF3D7\_1107800, PF3D7\_0613800, PF3D7\_0420300, and PF3D7\_1239200). The identification of PfSW1 and PfCHD1 in association with PfMORC strengthens the link between PfMORC and chromatin remodeling. This finding suggests that PfMORC may participate in regulating chromatin structure and gene expression during the IDC, notably the specific regulation of *var* genes. We note that some nuclear proteins were not identified in this study despite their documented interaction with PfMORC in other studies (Hillier et al., 2019; Bryant et al., 2020; Singh et al., 2021a, Subudhi et al., 2023). This may be due to differences in experimental conditions between the various studies and to the low abundance of the proteins. Despite this, our identification of several nuclear proteins in complex with PfMORC provides insights into potential interactions and

regulatory mechanisms underlying gene regulation and chromatin remodeling in *P. falciparum*; this may have implications for developing new strategies to combat malaria.

In other eukaryotes, MORC proteins function in gene repression and chromatin compaction at heterochromatic regions (Koch et al., 2017). Therefore, to determine if PfMORC localizes to heterochromatic regions across the *P. falciparum* genome, we performed ChIP-seq assays with PfMORC<sup>HA-glmS</sup> parasites during peak PfMORC expression (trophozoite and schizont stages). In general, PfMORC occupied regions 5'-upstream of the ATG start site or was bound within coding region, irrespective of the developmental stage. Most importantly, PfMORC peaks were reproducibly detected in subtelomeric regions containing hypervariable multigene families, including the var genes, consistent with the findings that PfMORC localized to var gene promoters as reported using dCas9 (Bryant et al., 2020). The specific binding pattern of PfMORC near or within PfHP1-bound regions suggests two related critical functions: heterochromatin condensation and gene repression. It is possible that PfMORC changes the nucleosome landscape either by direct association or by binding to different chromatin remodelers. Recent work in *Arabidopsis* has further confirmed the importance of AtMORC paralogs in gene regulation by chromatin compaction (Zhong et al., 2023), which resembles the function of PfMORC in *P. falciparum*. Interestingly, in *T. gondii*, the major function of TgMORC was in the repression of sex determination genes (Farhat et al., 2020), suggesting MORC family proteins have the capacity to perform diverse functions across eukaryotic organisms. Future studies should determine if PfMORC depletion similarly influences the rate of sexual commitment to *P. falciparum* gametocytogenesis, which is known to be regulated by epigenetic mechanisms. The role of PfHP1 has been shown in regulating sexual commitment by repressing PfAP2-G and virulence genes expression (Brancucci et al., 2014), whereas gametocyte development 1 (PFGDV1) displaces PfHP1 itself and induces asexual developing parasites to sexual differentiation (Filarsky et al., 2018).

We also compared PfMORC occupancy with available ChIP-seq data for the interacting ApiAP2 proteins. Interestingly, our analysis revealed a significant overlap between the binding sites of all ChIP-ed ApiAP2 proteins with PfMORC, suggesting a cooperative role in gene regulation. We also identified enriched motifs similar to those bound by our ApiAP2 proteins of interest, further suggesting the functional cooperation between PfMORC and ApiAP2 proteins. Of note, only one of the seven ApiAP2 of interest in our study has not been ChIP-ed to date (PF3D7\_0420300) (Shang et al., 2022). However, we found an enrichment of the DNA motif (TGCACACA) at PfMORC-bound sites. This motif is bound in vitro by PF3D7\_0420300 (Bonnell et al., 2023), suggesting that this ApiAP2 protein may localize to these regions. Overall, since these seven ApiAP2 proteins are expressed at distinct timepoints during the *P. falciparum* cycle (Bozdech et al., 2003) and regulate different sets of genes (Santos et al., 2017; Josling et al., 2020; Shang et al., 2021b; Shang et al., 2022; Subudhi et al., 2023), we believe this indicates a variety of functions for PfMORC at different stages. In addition, a recent study in *Arabidopsis* reported that AtMORC-mediated regulation of transcription may be due to both direct chromatin interactions and indirect association via sequence-specific transcription factors (Zhong et al., 2023) consistent with a complex landscape of chromatin remodeling by MORC proteins. We also interrogated the co-localization of PfMORC and numerous epigenetic profiles (H2A.Z, H3K9ac, H3K4me3, H3K27ac, H3K18ac, H3K9me3, H3K36me2/3, H4K20me3, and H3K4me1), with a specific focus on H3K36me2, since this histone modification has been shown to act as a global repressive effector in *P. falciparum* (Karmodiya et al., 2015) and other organisms (Strahl et al., 2002; Wagner and Carpenter, 2012). Interestingly, we did not find a strong co-localization with any of these epigenetic marks, suggesting a unique role of the epigenetic landscape on PfMORC global occupancy. Therefore, the functional association between PfMORC and a specific, unknown epigenetic mark remains to be determined.

Before this work, there was no direct evidence correlating PfMORC-mediated transcriptional changes during the IDC of *P. falciparum*. Therefore, we investigated the DEGs in PfMORC knockdown parasites and found two distinct subsets of enriched genes. The upregulated DEGs were enriched with genes related to invasion, while the downregulated DEGs belong to hypervariable genes associated with parasite virulence. It suggests that PfMORC has very dynamic function across *Plasmodium* asexual cycle as we also identified PfAP2-I in ColPed proteins, which is shown to regulate invasive gene transcription (Santos et al., 2017). Overall, our data with PfMORC-KD revealed a change in the expression of both antigenically variable and invasion-related genes. Expression of clonally variant genes occurs in a different but tightly regulated manner in IDC (Scherf et al., 1998; Scherf et al.,



2008), which, in the light of our data, may be regulated by PfMORC occupancy. Data regarding changes in *var* gene expression are difficult to interpret, as the KD experiments were performed on a parasite that had not been recloned and may therefore express more than one *var* gene. Single-cell experiments would be needed to clarify the effect of PfMORC KD on *var* gene regulation. We were surprised by the small number of DEGs detected upon knockdown of PfMORC, which we believe may be due to incomplete knockdown.

We previously showed that parasites in which PfMORC is knocked down display reduced sensitivity to melatonin (Singh *et al.*, 2021a). This prompted us to investigate if overall gene expression in PfMORC-KD parasites is affected by melatonin treatment. We detected only very slight changes (Figure 4—figure supplement 1), suggesting that melatonin does not exert its effect on gene expression through PfMORC, or at least that the latter protein plays a minor role in the process.

Overall, this study shows that PfMORC interacts with different ApiAP2 TFs, in line with previous studies (Hillier *et al.*, 2019; Bryant *et al.*, 2020; Singh *et al.*, 2021a, Subudhi *et al.*, 2023) and a recently published parallel study (Chahine *et al.*, 2023). Furthermore, we found that PfMORC is localized at sub-telomeric regions and contains significant overlap with the binding sites of several ApiAP2 transcription factors. Our results support a role for PfMORC in the regulation of hypervariable genes that are essential for *Plasmodium* virulence and rhoptry genes critical to RBC invasion. Collectively, our data identify an important role for PfMORC in chromatin organization, as well as in the epigenetic regulation of gene expression through regulatory complexes with an array of transcription factors, making it an attractive drug target.

## Materials and methods

### *Plasmodium falciparum* culture

The *P. falciparum* 3D7 strain (BEI Resources, MRA-102) and MORC constructs (3D7 background) were cultured at 37°C in RPMI 1640 medium supplemented with 0.5% Albumax II (Gibco) (Trager and Jensen, 1976). Parasites were grown under a 5% CO<sub>2</sub>, 5% O<sub>2</sub>, and 90% N<sub>2</sub> atmosphere. Cultures were synchronized with 5% sorbitol (Lambros and Vanderberg, 1979). Parasites were tested negative for mycoplasma contamination using PCR.

### Coimmunoprecipitation and mass spectrometry

Infected erythrocytes at the trophozoite stage were collected from culture and washed twice in 1× phosphate-buffered saline (PBS). The culture pellet was suspended in PBS containing 0.05% (w/v) saponin to lyse the erythrocyte membrane and centrifuged at 8000 × *g* for 10 min. The supernatant was discarded, and the parasite pellet was washed three times in cold PBS. To perform the co-immunoprecipitation, we followed the manufacturer's protocol (ChromoTek, gta-20). Samples were lysed in modified RIPA buffer (50 mM Tris, pH 7.5, 150 mM NaCl, 0.5% sodium deoxycholate, 1% Nonidet P-40, 10 µg/ml aprotinin, 10 µg/ml leupeptin, 10 µg/ml, 1 mM phenylmethylsulfonyl fluoride, benzamide) for 30 min on ice. The lysate was precleared with 50 µl of protein A/G-Agarose beads at 4°C for 1 hr and clarified by centrifugation at 10,000 × *g* for 10 min. The precleared lysate was incubated overnight with an anti-GFP-Trap-A beads (ChromoTek, gta-20) antibody. The magnetic beads were then pelleted using a magnet (Invitrogen), and the beads were washed extensively using wash buffer (50 mM Tris, pH 7.5, 150 mM NaCl, 0.5% sodium deoxycholate, 1% Nonidet P-40) to minimize the detection of non-specific proteins. To elute the immunoprecipitated proteins, the magnetic beads were resuspended in 2× SDS loading buffer and resolved by SDS-PAGE. Following SDS-PAGE, the whole gel band for each sample was excised from three independent experiments and further analyzed by mass spectrometry. We used a service provider (CEFAP core-facility de Espectometria de Massa) to analyze GFP-coimmunoprecipitated proteins.

### In-gel digestion and peptide desalting

Protein bands from polyacrylamide gels were cut into pieces (approximately 1 mm<sup>3</sup>), transferred to a clean 1.5 ml low binding tube and washed with washing solution (40% acetonitrile, 50 mM ammonium bicarbonate) until the bands were completely destained, and dehydrated with ACN 100% for 5 min



followed by vacuum centrifugation. Proteins were then reduced with 10 mM dithiothreitol in 50 mM ammonium bicarbonate and incubated for 45 min at 56°C. Protein alkylation was performed with 55 mM iodoacetamide in 50 mM ammonium bicarbonate and incubated for 30 min at room temperature. Proteins were digested into peptides by trypsin overnight reaction at 37°C. The trypsin reaction was stopped with 10% TFA (1% TFA final concentration). The supernatant was collected into a new tube. Extraction buffer (40% ACN/0.1% TFA) was added to the gel pieces and incubated for 15 min on a thermomixer at room temperature. The supernatant was transferred to the same microtube. The peptide extraction was performed twice and then dried in a vacuum centrifuge. Peptides were resuspended in 0.1% TFA for desalting.

### Nano LC-MS/MS analysis

The LC-MS/MS system employed was an Easy-nano LC 1200 system (Thermo Fisher Scientific Corp) coupled to an Orbitrap Fusion Lumos mass spectrometer equipped with a nanospray source (Thermo Fisher Scientific Corp). Samples were loaded onto a trapping column (Acclaim PepMap 0.075 mm, 2 cm, C18, 3 µm, 100 Å; Thermo Fisher Scientific Corp.) in line with a nano-LC column (Acclaim PepMap RSLC 0.050 mm, 15 cm, C18, 2 µm, 100 Å; Thermo Fisher Scientific Corp.). The gradient was 5–28% solvent B (A 0.1% FA; B 90% ACN, 0.1% FA) for 25 min, 28–40% B for 3 min, 40–95% B for 2 min, and 95% B for 12 min at 300 nl/min. Orbitrap Fusion Lumos mass spectrometer operated in positive mode. The full MS scan had an automatic gain control (AGC) of  $5 \times 10^5$  ions and a maximum filling time of 50 ms. Each MS scan was acquired at 120K full width half maximum high resolution in the Orbitrap with a mass range of  $m/z$  400–1600 Da. High-resolution dissociation with a normalized collision energy set at 30 was used for fragmentation. The resulting MS/MS fragment ions were detected in the Orbitrap mass analyzer at a resolution of 30,000. An AGC of  $5 \times 10^4$  ions and a maximum injection time of 54 ms were used. All raw data were accessed in Xcalibur software (Thermo Scientific).

### Database searches and bioinformatics analyses

Raw files were imported into MaxQuant version 1.6.17.0 for protein identification and quantification. For protein identification in MaxQuant, the database search engine Andromeda was used against the UniProt *P. falciparum* 3D7 strain (March 2021, 5388 entries release). The following parameters were used: carbamidomethylation of cysteine (57.021464 Da) as a fixed modification, oxidation of methionine (15.994915 Da), and N-terminal acetylation protein (42.010565 Da) were selected as variable modifications. Enzyme specificity was set to full trypsin with a maximum of two missed cleavages. The minimum peptide length was set to seven amino acids. For label-free quantification, the 'match between runs' feature in MaxQuant was used, which is able to identify the transfer between samples based on the retention time and accurate mass, with a 0.7 min match time window and 20 min alignment time window. Label-free quantification was performed using MaxQuant software with the 'match between run' and iBAQ features activated. Protein LFQ and iBAQ ratios were calculated for the two conditions, and the protein IDs were divided accordingly. The mass spectrometry proteomics data have been deposited to the ProteomeXchange Consortium via the PRIDE (Perez-Riverol et al., 2022) partner repository with the dataset identifier PXD036092. PlasmoDB database was used to perform GO analysis.

### Total RNA extraction and RNAseq

Infected RBCs containing tightly synchronized trophozoite stage parasites (32 hpi  $\pm$  3 hr) were harvested and resuspended in TRIzol (Thermo Fisher Scientific). Total RNA was extracted from three independent experiments following the manufacturer's protocol, and an RNA cleanup kit (QIAGEN) was used to achieve high-purity RNA. The isolated RNA was quantified using a NanoDrop ND-1000 UV/Vis spectrophotometer, and RNA quality was determined using an RNA ScreenTape System (Agilent 2200 TapeStation). Total RNA (10,000 ng) from each sample was stabilized in RNASTable (Biomatrix) and sent to the Micromon Genomics facility at Monash University for next-generation sequencing.

RNA samples were prepared using the MGITech RNA Directional Library Prep Kit V2 (Item No. 1000006385), as per the manufacturer's instructions, with the following parameters: input RNA: 50 ng, fragmentation: target of 200–400 bp, 87°C for 6 mins, adapter clean-up: 200–400 bp and

library amplification cycles: 16. Libraries were assessed for quantity using the Invitrogen Qubit and dsDNA HS chemistry (Item No. Q33230) and quality/quality using the Agilent Fragment Analyzer 5200 with the HS NGS Fragment Kit (Item No. DNF-473–0500). The libraries were pooled in equimolar concentrations and sequenced using an MGITech DNBSEQ-G400RS sequencing instrument with High-Throughput Sequencing Set (FCL PE100, Item No. 1000016950) chemistry.

The quality of the RNA-seq libraries was evaluated using the FastQC tool. Next, we used Salmon (V1.9.0) (Patro et al., 2017) quant with default arguments to quantify the expression of all transcripts in the PlasmoDB release-58 *Pfalciparum*3D7 genome. The transcript expression was summarized to gene-level expression with tximport 1.22.0 (Soneson et al., 2015). Finally, the gene counts were used to detect DEGs with DESeq2 (1.34.0) (Love et al., 2014). Furthermore, only genes with  $>1 \log_2$  fold change and adjusted  $p$ -value  $<0.1$  were considered significant for further analysis.

## Chromatin immunoprecipitation followed by high-throughput sequencing (ChIP-seq)

*PfMORC* ChIP-seq was performed similarly to previously published ChIP-seq experiments in *P. falciparum* (Josling et al., 2020; Singh et al., 2021a, Russell et al., 2022). Five samples in total were collected: biological duplicates using the *PfMORC*<sup>HA-glmS</sup> parasite line at the trophozoite stage (30 hpi), biological duplicates using the *PfMORC*<sup>HA</sup> parasite line at the schizont stage (40 hpi), and a single replicate using the *PfMORC*<sup>GFP</sup> parasite line at the schizont stage (40 hpi). In brief, the protocol includes five steps: (1) treated with 1% formaldehyde to crosslink the suspended *PfMORC*<sup>HA-glmS</sup> (or *PfMORC*<sup>GFP</sup>) parasite cultures (at least  $10^8$  trophozoite- or schizont-stage parasites synchronized with 10% sorbitol more than one cycle prior) at 37°C for 10 min; (2) collected parasite nuclei using prechilled glass Dounce homogenizer for 100 strokes per  $10^9$  trophozoites/schizonts; (3) lysed parasite nuclei and mechanically sheared chromatin until sufficiently sheared using Covaris Focus-Ultrasonicator M220 (5% duty cycle, 75 W peak incident power, 200 cycles per burst, 7°C, for 5 min). (4) We collected 10% of each sample for the non-immunoprecipitated 'input' control and then immunoprecipitated the remaining 90% of each sample. The remaining 90% of each sample was immunoprecipitated with 1:1000 anti-HA antibody (0.5 mg/ml Roche Rat Anti-HA High Affinity [11867423001]) or 1:1000 anti-GFP antibody (0.1 mg/ml Abcam Rabbit Anti-GFP [Ab290]) overnight at 4°C with rotation. (5) DNA was purified after reverse crosslinking using a MinElute column (QIAGEN) as directed and quantified by a Qubit fluorometer (Invitrogen).

## ChIP-seq library prep for Illumina sequencing

The *PfMORC* ChIP-seq libraries were performed similarly to previously published ChIP-seq experiments in *P. falciparum* (Josling et al., 2020; Singh et al., 2021b, Russell et al., 2022). DNA sequencing libraries were prepared for high-throughput Illumina sequencing on the NextSeq 2000 with the 150 × 150 single-end mode. The library prep underwent 12 rounds of amplification using KAPA HiFi polymerase. Completed libraries were quantified using the Qubit fluorometer (Invitrogen) for high-sensitivity DNA and library sequence length by the Agilent TapeStation 4150.

## ChIP-seq data analysis and peak calling

The *PfMORC* ChIP-seq datasets were analyzed similar to previously published ChIP-seq experiments in *P. falciparum* (Josling et al., 2020; Singh et al., 2021b, Russell et al., 2022). Raw sequencing reads were trimmed (Trimomatic v0.32.3) to remove Illumina adaptor sequences and low-quality reads below 30 Phred (SLIDINGWINDOW: 4:30). FastQC (v0.11.9) was used to check the quality after trimming. Processed reads were then mapped to the *P. falciparum* genome (release 57) using BWA-MEM (v0.7.17.2) simple Illumina mode with multiple mapped reads filtered out (MAPQ = 1). Once the sequences were mapped, MACS2 (v2.2.7.1) was used to call peaks with each biological replicate and its paired input sample using a standard significance cutoff ( $q$ -value = 0.01). Using BedTools Multiple Intersect (v2.29.2), the narrow peak output file for each replicate was overlapped to identify the significant peaks in the overlap between both ChIP-seq biological replicates. The overlapping regions were then used to identify an enriched DNA motif (STREME Meme Suite: Bailey, 2021), and putative gene targets of *PfMORC* were defined as genes with peaks within 2 kb upstream of the gene target ATG start codon or peaks within gene bodies. In a situation with any peaks between gene targets in a head-to-head orientation, the closest gene was chosen.

## Acknowledgements

This work was supported by grants from Fundação de Amparo a Pesquisa de São Paulo (FAPESP) to CRSG (2017/08684-7 and 2018/07177-7) and to MKS (2019/09490-7). CRSG is supported by 'bolsa de produtividade' by CNPq. This work was supported by the National Institutes of Health grant number R01-AI125565 to ML and T32-GM125592 to VAB. We are grateful to Haemocentro Hospital do Servidor Público for providing blood and plasma. Work in CD laboratory is supported by RMIT University and by grant APP2003712 from the Australian Health and Medical Research Council (NHMRC). We thank Prof. Paolo Di Mascio and Graziella E Ronsein for the Mass spectrometry analyses performed at the Redox Proteomics Core of the Mass Spectrometry Resource at Chemistry Institute, University of São Paulo (FAPESP 2012/12663-1, 2016/00696-3, 2023/00995-4, CEPID Redoxoma 2013/07937-8), and Dr. Mariana P Massafera for her technical assistance.

## Additional information

### Funding

Funder	Grant reference number	Author
Fundação de Amparo à Pesquisa do Estado de São Paulo	2017/08684-7	Celia RS Garcia
Fundação de Amparo à Pesquisa do Estado de São Paulo	2018/07177-7	Celia RS Garcia
Fundação de Amparo à Pesquisa do Estado de São Paulo	2019/09490-7	Maneesh Kumar Singh
National Institutes of Health	R01-AI125565	Manuel Llinas
National Institutes of Health	T32-GM125592	Victoria Ann Bonnell
National Health and Medical Research Council	APP2003712	Christian Doerig

The funders had no role in study design, data collection and interpretation, or the decision to submit the work for publication.


### Author contributions

Maneesh Kumar Singh, Conceptualization, Data curation, Formal analysis, Investigation, Methodology, Writing – original draft, Writing – review and editing; Victoria Ann Bonnell, Conceptualization, Data curation, Methodology, Writing – original draft; Israel Tojal Da Silva, Formal analysis; Verônica Feijoli Santiago, Investigation, Methodology; Miriam Santos Moraes, Methodology; Jack Adderley, Resources; Christian Doerig, Conceptualization, Resources, Supervision, Project administration, Writing – review and editing; Giuseppe Palmisano, Supervision, Project administration, Writing – review and editing; Manuel Llinas, Conceptualization, Supervision, Funding acquisition, Project administration, Writing – review and editing; Celia RS Garcia, Conceptualization, Resources, Supervision, Funding acquisition, Project administration, Writing – review and editing


### Author ORCIDs

Maneesh Kumar Singh  <https://orcid.org/0000-0003-1474-4695>

Israel Tojal Da Silva  <https://orcid.org/0000-0002-4687-1499>

Verônica Feijoli Santiago  <https://orcid.org/0000-0002-0052-9532>

Christian Doerig  <https://orcid.org/0000-0002-3188-094X>

Giuseppe Palmisano  <https://orcid.org/0000-0003-1336-6151>

Manuel Llinas  <https://orcid.org/0000-0002-6173-5882>

Celia RS Garcia  <https://orcid.org/0000-0003-2825-1701>

## Peer review material

Reviewer #1 (Public Review): <https://doi.org/10.7554/eLife.92201.3.sa1>Author response <https://doi.org/10.7554/eLife.92201.3.sa2>

## Additional files

## Supplementary files

- Supplementary file 1. Intersecting peptide hits from three different experiments obtained from PfMORC-GFP parasite lysate.
- Supplementary file 2. Complete list of potential PfMORC interacting proteins enriched in ColP eluates and identified in LC-MS/MS from three independent experiments and fold change  $\geq 1.5 \times$  GFP/3D7.
- Supplementary file 3. Gene Ontology (GO) terms for proteins identified in PfMORC-GFP lysate and normalized to fold change  $> 1.5$ .
- Supplementary file 4. Gene IDs and annotations for gene targets of PfMORC at 30 hpi and 40 hpi determined by ChIP-seq genome-wide occupancy. Putative gene targets of PfMORC were defined as genes with peaks within 2 kb upstream of the gene target ATG start codon or peaks within gene bodies. In a situation with any peaks between gene targets in a head-to-head orientation, the closest gene was chosen.
- Supplementary file 5. Gene Ontology (GO) terms for gene targets of PfMORC at 30 hpi and 40 hpi determined by ChIP-seq genome-wide occupancy. GO Terms were defined using [PlasmoDB.org](https://plasmodb.org) GO Term enrichment function (Biological Process with p-value cutoff of 0.05).
- Supplementary file 6. Full list of differentially expressed genes in PfMORC-KD vs. PfMORC-WT.
- Supplementary file 7. Gene Ontology (GO) terms for differentially expressed genes identified in PfMORC-KD/PfMORC-WT RNAseq.
- Supplementary file 8. List of differentially expressed genes in PfMORC-KD vs. PfMORC-WT after 100 nM melatonin treatment for 5 hr.
- MDAR checklist

## Data availability

The proteomics data have been deposited to the ProteomeXchange Consortium via the PRIDE partner repository with the dataset identifier PXD044256. All ChIP-seq samples were submitted to GEO under accession code GSE239393. All RNA-seq samples were submitted to GEO under accession code GSE241313.

The following datasets were generated:

Author(s)	Year	Dataset title	Dataset URL	Database and Identifier
Santiago VF, Garcia CRS	2024	<i>Plasmodium falciparum</i> MORC protein modulates gene expression through interaction with heterochromatin	<a href="https://proteomecentral.proteomexchange.org/cgi/GetDataset?ID=PX044256">https://proteomecentral.proteomexchange.org/cgi/GetDataset?ID=PX044256</a>	ProteomeXchange, PXD044256
Singh MK, Bonnell VA, Tojal da Silva I, Santiago VF, Moraes MS, Adderley J, Doerig C, Llinás M, Garcia CRG	2024	PfMORC modulates gene expression through interactions with heterochromatin in <i>Plasmodium falciparum</i>	<a href="https://www.ncbi.nlm.nih.gov/geo/query/acc.cgi?acc=GSE239393">https://www.ncbi.nlm.nih.gov/geo/query/acc.cgi?acc=GSE239393</a>	NCBI Gene Expression Omnibus, GSE239393
Singh M, Tojal da Silva I, Adderley J, Doerig C, da Silva Garcia C	2023	<i>Plasmodium falciparum</i> MORC protein modulates gene expression through interaction with heterochromatin	<a href="https://www.ncbi.nlm.nih.gov/geo/query/acc.cgi?acc=GSE241313">https://www.ncbi.nlm.nih.gov/geo/query/acc.cgi?acc=GSE241313</a>	NCBI Gene Expression Omnibus, GSE241313

## References

- Antunes AV**, Shahinas M, Swale C, Farhat DC, Ramakrishnan C, Bruley C, Cannella D, Robert MG, Corrao C, Couté Y, Hehl AB, Bougdour A, Coppens I, Hakimi M-A. 2024. In vitro production of cat-restricted *Toxoplasma* pre-sexual stages. *Nature* **625**:366–376. DOI: <https://doi.org/10.1038/s41586-023-06821-y>, PMID: 38093015
- Arastu-Kapur S**, Ponder EL, Fonović UP, Yeoh S, Yuan F, Fonović M, Grainger M, Phillips CI, Powers JC, Bogyo M. 2008. Identification of proteases that regulate erythrocyte rupture by the malaria parasite *Plasmodium falciparum*. *Nature Chemical Biology* **4**:203–213. DOI: <https://doi.org/10.1038/nchembio.70>, PMID: 18246061
- Bailey TL**. 2021. STREME: accurate and versatile sequence motif discovery. *Bioinformatics* **37**:2834–2840. DOI: <https://doi.org/10.1093/bioinformatics/btab203>, PMID: 33760053
- Balaji S**, Babu MM, Iyer LM, Aravind L. 2005. Discovery of the principal specific transcription factors of Apicomplexa and their implication for the evolution of the AP2-integrase DNA binding domains. *Nucleic Acids Research* **33**:3994–4006. DOI: <https://doi.org/10.1093/nar/gki709>, PMID: 16040597
- Bonnell VA**, Zhang Y, Brown JAS, Horton J, Josling GA, Chiu TP, Rohs R, Mahony S, Gordán R, Llinás M. 2023. DNA Sequence context and the chromatin landscape differentiate sequence-specific transcription factor binding in the human malaria parasite, *Plasmodium falciparum*. *bioRxiv*. DOI: <https://doi.org/10.1101/2023.03.31.535174>
- Bordiya Y**, Zheng Y, Nam JC, Bonnard AC, Choi HW, Lee BK, Kim J, Klessig DF, Fei Z, Kang HG. 2016. Pathogen infection and morc proteins affect chromatin accessibility of transposable elements and expression of their proximal genes in arabidopsis. *Molecular Plant-Microbe Interactions* **29**:674–687. DOI: <https://doi.org/10.1094/MPMI-01-16-0023-R>, PMID: 27482822
- Bozdech Z**, Llinás M, Pulliam BL, Wong ED, Zhu J, DeRisi JL. 2003. The transcriptome of the intraerythrocytic developmental cycle of *Plasmodium falciparum*. *PLOS Biology* **1**:E5. DOI: <https://doi.org/10.1371/journal.pbio.0000005>, PMID: 12929205
- Brancucci NMB**, Bertschi NL, Zhu L, Niederwieser I, Chin WH, Wampfler R, Freymond C, Rottmann M, Felger I, Bozdech Z, Voss TS. 2014. Heterochromatin protein 1 secures survival and transmission of malaria parasites. *Cell Host & Microbe* **16**:165–176. DOI: <https://doi.org/10.1016/j.chom.2014.07.004>, PMID: 25121746
- Bryant JM**, Baumgarten S, Dingli F, Loew D, Sinha A, Claës A, Preiser PR, Dedon PC, Scherf A. 2020. Exploring the virulence gene interactome with CRISPR/dCas9 in the human malaria parasite. *Molecular Systems Biology* **16**:e9569. DOI: <https://doi.org/10.15252/msb.20209569>, PMID: 32816370
- Bushell E**, Gomes AR, Sanderson T, Anar B, Girling G, Herd C, Metcalf T, Modrzynska K, Schwach F, Martin RE, Mather MW, McFadden GI, Parts L, Rutledge GG, Vaidya AB, Wengelnik K, Rayner JC, Billker O. 2017. Functional profiling of a plasmodium genome reveals an abundance of essential genes. *Cell* **170**:260–272. DOI: <https://doi.org/10.1016/j.cell.2017.06.030>, PMID: 28708996
- Campbell TL**, De Silva EK, Olszewski KL, Elemento O, Llinás M. 2010. Identification and genome-wide prediction of DNA binding specificities for the ApiAP2 family of regulators from the malaria parasite. *PLOS Pathogens* **6**:e1001165. DOI: <https://doi.org/10.1371/journal.ppat.1001165>, PMID: 21060817
- Carrington E**, Cooijmans RHM, Keller D, Toenhake CG, Bártfai R, Voss TS. 2021. The ApiAP2 factor PfAP2-HC is an integral component of heterochromatin in the malaria parasite *Plasmodium falciparum*. *iScience* **24**:102444. DOI: <https://doi.org/10.1016/j.isci.2021.102444>, PMID: 33997710
- Chahine Z**, Gupta M, Lenz T, Hollin T, Abel S, Banks C, Saraf A, Prudhomme J, Florens L, Le Roch K. 2023. PfMORC Protein regulates chromatin accessibility and transcriptional repression in the human malaria parasite, *P. falciparum*. *bioRxiv*. DOI: <https://doi.org/10.1101/2023.09.11.557253>
- Chappell L**, Ross P, Orchard L, Russell TJ, Otto TD, Berriman M, Rayner JC, Llinás M. 2020. Refining the transcriptome of the human malaria parasite *Plasmodium falciparum* using amplification-free RNA-seq. *BMC Genomics* **21**:395. DOI: <https://doi.org/10.1186/s12864-020-06787-5>, PMID: 32513207
- Cowman AF**, Berry D, Baum J. 2012. The cellular and molecular basis for malaria parasite invasion of the human red blood cell. *The Journal of Cell Biology* **198**:961–971. DOI: <https://doi.org/10.1083/jcb.201206112>, PMID: 22986493
- Dong W**, Vannozzi A, Chen F, Hu Y, Chen Z, Zhang L. 2018. MORC domain definition and evolutionary analysis of the MORC gene family in green plants. *Genome Biology and Evolution* **10**:1730–1744. DOI: <https://doi.org/10.1093/gbe/evy136>, PMID: 29982569
- Farhat DC**, Swale C, Dard C, Cannella D, Ortet P, Barakat M, Sindikubwabo F, Belmudes L, De Bock PJ, Couté Y, Bougdour A, Hakimi MA. 2020. A MORC-driven transcriptional switch controls *Toxoplasma* developmental trajectories and sexual commitment. *Nature Microbiology* **5**:570–583. DOI: <https://doi.org/10.1038/s41564-020-0674-4>, PMID: 32094587
- Filarsky M**, Fraschka SA, Niederwieser I, Brancucci NMB, Carrington E, Carrió E, Moes S, Jenoe P, Bártfai R, Voss TS. 2018. GDV1 induces sexual commitment of malaria parasites by antagonizing HP1-dependent gene silencing. *Science* **359**:1259–1263. DOI: <https://doi.org/10.1126/science.aan6042>, PMID: 29590075
- Flueck C**, Bártfai R, Niederwieser I, Witmer K, Alako BTF, Moes S, Bozdech Z, Jenoe P, Stunnenberg HG, Voss TS. 2010. A major role for the *Plasmodium falciparum* ApiAP2 protein PfSIP2 in chromosome end biology. *PLOS Pathogens* **6**:e1000784. DOI: <https://doi.org/10.1371/journal.ppat.1000784>, PMID: 20195509
- Fraschka SA**, Filarsky M, Hoo R, Niederwieser I, Yam XY, Brancucci NMB, Mohring F, Mushunje AT, Huang X, Christensen PR, Nosten F, Bozdech Z, Russell B, Moon RW, Marti M, Preiser PR, Bártfai R, Voss TS. 2018. Comparative heterochromatin profiling reveals conserved and unique epigenome signatures linked to



- adaptation and development of malaria parasites. *Cell Host & Microbe* **23**:407–420. DOI: <https://doi.org/10.1016/j.chom.2018.01.008>, PMID: 29503181
- Gardner MJ**, Hall N, Fung E, White O, Berriman M, Hyman RW, Carlton JM, Pain A, Nelson KE, Bowman S, Paulsen IT, James K, Eisen JA, Rutherford K, Salzberg SL, Craig A, Kyes S, Chan MS, Nene V, Shallom SJ, et al. 2002. Genome sequence of the human malaria parasite *Plasmodium falciparum*. *Nature* **419**:498–511. DOI: <https://doi.org/10.1038/nature01097>, PMID: 12368864
- Guizetti J**, Scherf A. 2013. Silence, activate, poise and switch! Mechanisms of antigenic variation in *Plasmodium falciparum*. *Cellular Microbiology* **15**:718–726. DOI: <https://doi.org/10.1111/cmi.12115>, PMID: 23351305
- Harris MT**, Jeffers V, Martynowicz J, True JD, Mosley AL, Sullivan WJ. 2019. A novel GCN5b lysine acetyltransferase complex associates with distinct transcription factors in the protozoan parasite *Toxoplasma gondii*. *Molecular and Biochemical Parasitology* **232**:111203. DOI: <https://doi.org/10.1016/j.molbiopara.2019.111203>, PMID: 31381949
- Hillier C**, Pardo M, Yu L, Bushell E, Sanderson T, Metcalf T, Herd C, Anar B, Rayner JC, Billker O, Choudhary JS. 2019. Landscape of the Plasmodium Interactome reveals both conserved and species-specific functionality. *Cell Reports* **28**:1635–1647. DOI: <https://doi.org/10.1016/j.celrep.2019.07.019>, PMID: 31390575
- Hoeijmakers WAM**, Miao J, Schmidt S, Toenhake CG, Shrestha S, Venhuizen J, Henderson R, Birnbaum J, Ghidelli-Disse S, Drewes G, Cui L, Stunnenberg HG, Spielmann T, Bártfai R. 2019. Epigenetic reader complexes of the human malaria parasite, *Plasmodium falciparum*. *Nucleic Acids Research* **47**:11574–11588. DOI: <https://doi.org/10.1093/nar/gkz1044>, PMID: 31728527
- Hollin T**, Gupta M, Lenz T, Le Roch KG. 2021. Dynamic chromatin structure and epigenetics control the fate of malaria parasites. *Trends in Genetics* **37**:73–85. DOI: <https://doi.org/10.1016/j.tig.2020.09.003>, PMID: 32988634
- Iyer LM**, Abhiman S, Aravind L. 2008a. MutL homologs in restriction-modification systems and the origin of eukaryotic MORC ATPases. *Biology Direct* **3**:8. DOI: <https://doi.org/10.1186/1745-6150-3-8>, PMID: 18346280
- Iyer LM**, Anantharaman V, Wolf MY, Aravind L. 2008b. Comparative genomics of transcription factors and chromatin proteins in parasitic protists and other eukaryotes. *International Journal for Parasitology* **38**:1–31. DOI: <https://doi.org/10.1016/j.ijpara.2007.07.018>, PMID: 17949725
- Jenina MD**, Quinn JE, Petter M. 2019. ApiAP2 transcription factors in apicomplexan parasites. *Pathogens* **8**:47. DOI: <https://doi.org/10.3390/pathogens8020047>, PMID: 30959972
- Jiang L**, Mu J, Zhang Q, Ni T, Srinivasan P, Rayavara K, Yang W, Turner L, Lavstsen T, Theander TG, Peng W, Wei G, Jing Q, Wakabayashi Y, Bansal A, Luo Y, Ribeiro JMC, Scherf A, Aravind L, Zhu J, et al. 2013. PfSETvs methylation of histone H3K36 represses virulence genes in *Plasmodium falciparum*. *Nature* **499**:223–227. DOI: <https://doi.org/10.1038/nature12361>, PMID: 23823717
- Josling GA**, Russell TJ, Venezia J, Orchar L, van Biljon R, Painter HJ, Llinás M. 2020. Dissecting the role of PfAP2-G in malaria gametocytogenesis. *Nature Communications* **11**:1503. DOI: <https://doi.org/10.1038/s41467-020-15026-0>, PMID: 32198457
- Kafsack BFC**, Rovira-Graells N, Clark TG, Bancells C, Crowley VM, Campino SG, Williams AE, Drought LG, Kwiatkowski DP, Baker DA, Cortés A, Llinás M. 2014. A transcriptional switch underlies commitment to sexual development in malaria parasites. *Nature* **507**:248–252. DOI: <https://doi.org/10.1038/nature12920>, PMID: 24572369
- Kang HG**, Hyong WC, von Einem S, Manosalva P, Ehlers K, Liu PP, Buxa SV, Moreau M, Mang HG, Kachroo P, Kogel KH, Klessig DF. 2012. CRT1 is a nuclear-translocated MORC endonuclease that participates in multiple levels of plant immunity. *Nature Communications* **3**:1297. DOI: <https://doi.org/10.1038/ncomms2279>, PMID: 23250427
- Karmodiya K**, Pradhan SJ, Joshi B, Jangid R, Reddy PC, Galande S. 2015. A comprehensive epigenome map of *Plasmodium falciparum* reveals unique mechanisms of transcriptional regulation and identifies H3K36me2 as a global mark of gene suppression. *Epigenetics & Chromatin* **8**:32. DOI: <https://doi.org/10.1186/s13072-015-0029-1>, PMID: 26388940
- Kim H**, Yen L, Wongpalee SP, Kirshner JA, Mehta N, Xue Y, Johnston JB, Burlingame AL, Kim JK, Loparo JJ, Jacobsen SE. 2019. The Gene-Silencing Protein MORC-1 Topologically Entraps DNA and Forms Multimeric Assemblies to Cause DNA Compaction. *Molecular Cell* **75**:700–710. DOI: <https://doi.org/10.1016/j.molcel.2019.07.032>, PMID: 31442422
- Koch A**, Kang HG, Steinbrenner J, Dempsey DA, Klessig DF, Kogel KH. 2017. MORC Proteins: Novel Players in Plant and Animal Health. *Frontiers in Plant Science* **8**:1720. DOI: <https://doi.org/10.3389/fpls.2017.01720>, PMID: 29093720
- Lambros C**, Vanderberg JP. 1979. Synchronization of *Plasmodium falciparum* erythrocytic stages in culture. *The Journal of Parasitology* **65**:418–420. PMID: 383936.
- Le Roch KG**, Zhou Y, Blair PL, Grainger M, Moch JK, Haynes JD, De La Vega P, Holder AA, Batalov S, Carucci DJ, Winzeler EA. 2003. Discovery of gene function by expression profiling of the malaria parasite life cycle. *Science* **301**:1503–1508. DOI: <https://doi.org/10.1126/science.1087025>, PMID: 12893887
- Love MI**, Huber W, Anders S. 2014. Moderated estimation of fold change and dispersion for RNA-seq data with DESeq2. *Genome Biology* **15**:550. DOI: <https://doi.org/10.1186/s13059-014-0550-8>, PMID: 25516281
- Miao J**, Wang C, Lucky AB, Liang X, Min H, Adapa SR, Jiang R, Kim K, Cui L. 2021. A unique GCN5 histone acetyltransferase complex controls erythrocyte invasion and virulence in the malaria parasite *Plasmodium falciparum*. *PLOS Pathogens* **17**:e1009351. DOI: <https://doi.org/10.1371/journal.ppat.1009351>, PMID: 34403450
- Modrzynska K**, Pfander C, Chappell L, Yu L, Suarez C, Dundas K, Gomes AR, Goulding D, Rayner JC, Choudhary J, Billker O. 2017. A Knockout Screen of ApiAP2 Genes Reveals Networks of Interacting

- Transcriptional Regulators Controlling the Plasmodium Life Cycle. *Cell Host & Microbe* **21**:11–22. DOI: <https://doi.org/10.1016/j.chom.2016.12.003>, PMID: 28081440
- Moissiard G**, Cokus SJ, Cary J, Feng S, Billi AC, Stroud H, Husmann D, Zhan Y, Lajoie BR, McCord RP, Hale CJ, Feng W, Michaels SD, Frand AR, Pellegrini M, Dekker J, Kim JK, Jacobsen SE. 2012. MORC family ATPases required for heterochromatin condensation and gene silencing. *Science* **336**:1448–1451. DOI: <https://doi.org/10.1126/science.1221472>, PMID: 22555433
- Painter HJ**, Campbell TL, Llinás M. 2011. The Apicomplexan AP2 family: integral factors regulating Plasmodium development. *Molecular and Biochemical Parasitology* **176**:1–7. DOI: <https://doi.org/10.1016/j.molbiopara.2010.11.014>, PMID: 21126543
- Patro R**, Duggal G, Love MI, Irizarry RA, Kingsford C. 2017. Salmon provides fast and bias-aware quantification of transcript expression. *Nature Methods* **14**:417–419. DOI: <https://doi.org/10.1038/nmeth.4197>, PMID: 28263959
- Perez-Riverol Y**, Bai J, Bandla C, García-Seisdedos D, Hewapathirana S, Kamatchinathan S, Kundu DJ, Prakash A, Frericks-Zipper A, Eisenacher M, Walzer M, Wang S, Brazma A, Vizcaíno JA. 2022. The PRIDE database resources in 2022: a hub for mass spectrometry-based proteomics evidences. *Nucleic Acids Research* **50**:D543–D552. DOI: <https://doi.org/10.1093/nar/gkab1038>, PMID: 34723319
- Pradhan A**, Chauhan VS, Tuteja R. 2005. *Plasmodium falciparum* DNA helicase 60 is a schizont stage specific, bipolar and dual helicase stimulated by PKC phosphorylation. *Molecular and Biochemical Parasitology* **144**:133–141. DOI: <https://doi.org/10.1016/j.molbiopara.2005.08.006>, PMID: 16165232
- Quinn JE**, Jenning MD, Limm K, Pareek K, Meißgeier T, Bachmann A, Duffy MF, Petter M. 2022. The Putative Bromodomain Protein PfBDP7 of the Human Malaria Parasite *Plasmodium Falciparum* Cooperates With PfBDP1 in the Silencing of Variant Surface Antigen Expression. *Frontiers in Cell and Developmental Biology* **10**:816558. DOI: <https://doi.org/10.3389/fcell.2022.816558>, PMID: 35493110
- Real E**, Nardella F, Scherf A, Mancio-Silva L. 2022. Repurposing of *Plasmodium falciparum* var genes beyond the blood stage. *Current Opinion in Microbiology* **70**:102207. DOI: <https://doi.org/10.1016/j.mib.2022.102207>, PMID: 36183663
- Russell TJ**, De Silva EK, Crowley VM, Shaw-Saliba K, Dube N, Josling G, Pasaje CFA, Kouskoumvekaki I, Panagiotou G, Niles JC, Jacobs-Lorena M, Denise Okafor C, Gamo FJ, Llinás M. 2022. Inhibitors of ApiAP2 protein DNA binding exhibit multistage activity against Plasmodium parasites. *PLOS Pathogens* **18**:e1010887. DOI: <https://doi.org/10.1371/journal.ppat.1010887>, PMID: 36223427
- Santos JM**, Josling G, Ross P, Joshi P, Orchard L, Campbell T, Schieler A, Cristea IM, Llinás M. 2017. Red Blood Cell Invasion by the Malaria Parasite Is Coordinated by the PfAP2-I Transcription Factor. *Cell Host & Microbe* **21**:731–741. DOI: <https://doi.org/10.1016/j.chom.2017.05.006>, PMID: 28618269
- Sargeant TJ**, Marti M, Caler E, Carlton JM, Simpson K, Speed TP, Cowman AF. 2006. Lineage-specific expansion of proteins exported to erythrocytes in malaria parasites. *Genome Biology* **7**:R12. DOI: <https://doi.org/10.1186/gb-2006-7-2-r12>, PMID: 16507167
- Scherf A**, Hernandez-Rivas R, Buffet P, Bottius E, Benatar C, Pouvelle B, Gysin J, Lanzer M. 1998. Antigenic variation in malaria: in situ switching, relaxed and mutually exclusive transcription of var genes during intraerythrocytic development in *Plasmodium falciparum*. *The EMBO Journal* **17**:5418–5426. DOI: <https://doi.org/10.1093/emboj/17.18.5418>, PMID: 9736619
- Scherf A**, Lopez-Rubio JJ, Riviere L. 2008. Antigenic variation in *Plasmodium falciparum*. *Annual Review of Microbiology* **62**:445–470. DOI: <https://doi.org/10.1146/annurev.micro.61.080706.093134>, PMID: 18785843
- Schneider VM**, Visone JE, Harris CT, Florini F, Hadjimichael E, Zhang X, Gross MR, Rhee KY, Ben Mamoun C, Kafsack BFC, Deitsch KW. 2023. The human malaria parasite *Plasmodium falciparum* can sense environmental changes and respond by antigenic switching. *PNAS* **120**:e2302152120. DOI: <https://doi.org/10.1073/pnas.2302152120>, PMID: 37068249
- Shang X**, Shen S, Tang J, He X, Zhao Y, Wang C, He X, Guo G, Liu M, Wang L, Zhu Q, Yang G, Jiang C, Zhang M, Yu X, Han J, Culleton R, Jiang L, Cao J, Gu L, et al. 2021a. A cascade of transcriptional repression determines sexual commitment and development in *Plasmodium falciparum*. *Nucleic Acids Research* **49**:9264–9279. DOI: <https://doi.org/10.1093/nar/gkab683>, PMID: 34365503
- Shang X**, Wang C, Shen L, Sheng F, He X, Wang F, Fan Y, He X, Jiang M. 2021b. PfAP2-EXP2, an essential transcription factor for the intraerythrocytic development of *Plasmodium falciparum*. *Frontiers in Cell and Developmental Biology* **9**:782293. DOI: <https://doi.org/10.3389/fcell.2021.782293>, PMID: 35083215
- Shang X**, Wang C, Fan Y, Guo G, Wang F, Zhao Y, Sheng F, Tang J, He X, Yu X, Zhang M, Zhu G, Yin S, Mu J, Culleton R, Cao J, Jiang M, Zhang Q. 2022. Genome-wide landscape of ApiAP2 transcription factors reveals a heterochromatin-associated regulatory network during *Plasmodium falciparum* blood-stage development. *Nucleic Acids Research* **50**:3413–3431. DOI: <https://doi.org/10.1093/nar/gkac176>, PMID: 35288749
- Sierra-Miranda M**, Vembar SS, Delgadillo DM, Ávila-López PA, Herrera-Solorio AM, Lozano Amado D, Vargas M, Hernandez-Rivas R. 2017. PfAP2Tel, harbouring a non-canonical DNA-binding AP2 domain, binds to *Plasmodium falciparum* telomeres. *Cellular Microbiology* **19**:12742. DOI: <https://doi.org/10.1111/cmi.12742>, PMID: 28376558
- Singh S**, Alam MM, Pal-Bhowmick I, Brzostowski JA, Chitnis CE. 2010. Distinct external signals trigger sequential release of apical organelles during erythrocyte invasion by malaria parasites. *PLOS Pathogens* **6**:e1000746. DOI: <https://doi.org/10.1371/journal.ppat.1000746>, PMID: 20140184
- Singh S**, Santos JM, Orchard LM, Yamada N, van Bijljon R, Painter HJ, Mahony S, Llinás M. 2021a. The PfAP2-G2 transcription factor is a critical regulator of gametocyte maturation. *Molecular Microbiology* **115**:1005–1024. DOI: <https://doi.org/10.1111/mmi.14676>, PMID: 33368818

- Singh MK**, Tessarin-Almeida G, Dias BKM, Pereira PS, Costa F, Przyborski JM, Garcia CRS. 2021b. A nuclear protein, PflMORC confers melatonin dependent synchrony of the human malaria parasite *P. falciparum* in the asexual stage. *Scientific Reports* **11**:2057. DOI: <https://doi.org/10.1038/s41598-021-81235-2>, PMID: 33479315
- Sinha A**, Hughes KR, Modrzynska KK, Otto TD, Pfander C, Dickens NJ, Religa AA, Bushell E, Graham AL, Cameron R, Kafsack BFC, Williams AE, Llinas M, Berriman M, Billker O, Waters AP. 2014. A cascade of DNA-binding proteins for sexual commitment and development in *Plasmodium*. *Nature* **507**:253–257. DOI: <https://doi.org/10.1038/nature12970>, PMID: 24572359
- Smith LM**, Motta FC, Chopra G, Moch JK, Nerem RR, Cummins B, Roche KE, Kelliher CM, Leman AR, Harer J, Gedeon T, Waters NC, Haase SB. 2020. An intrinsic oscillator drives the blood stage cycle of the malaria parasite *Plasmodium falciparum*. *Science* **368**:754–759. DOI: <https://doi.org/10.1126/science.aba4357>, PMID: 32409472
- Soneson C**, Love MI, Robinson MD. 2015. Differential analyses for RNA-seq: transcript-level estimates improve gene-level inferences. *F1000Research* **4**:1521. DOI: <https://doi.org/10.12688/f1000research.7563.2>, PMID: 26925227
- Srinivasan P**, Yasgar A, Luci DK, Beatty WL, Hu X, Andersen J, Narum DL, Moch JK, Sun H, Haynes JD, Maloney DJ, Jadhav A, Simeonov A, Miller LH. 2013. Disrupting malaria parasite AMA1-RON2 interaction with a small molecule prevents erythrocyte invasion. *Nature Communications* **4**:2261. DOI: <https://doi.org/10.1038/ncomms3261>, PMID: 23907321
- Srivastava S**, Holmes MJ, White MW, Sullivan WJ. 2023. *Toxoplasma gondii* AP2XII-2 Contributes to Transcriptional Repression for Sexual Commitment. *mSphere* **8**:e0060622. DOI: <https://doi.org/10.1128/msphere.00606-22>, PMID: 36786611
- Strahl BD**, Grant PA, Briggs SD, Sun ZW, Bone JR, Caldwell JA, Mollah S, Cook RG, Shabanowitz J, Hunt DF, Allis CD. 2002. Set2 is a nucleosomal histone H3-selective methyltransferase that mediates transcriptional repression. *Molecular and Cellular Biology* **22**:1298–1306. DOI: <https://doi.org/10.1128/MCB.22.5.1298-1306.2002>, PMID: 11839797
- Subudhi AK**, O'Donnell AJ, Ramaprasad A, Abkallo HM, Kaushik A, Ansari HR, Abdel-Haleem AM, Ben Rached F, Kaneko O, Culleton R, Reece SE, Pain A. 2020. Malaria parasites regulate intra-erythrocytic development duration via serpentine receptor 10 to coordinate with host rhythms. *Nature Communications* **11**:2763. DOI: <https://doi.org/10.1038/s41467-020-16593-y>, PMID: 32488076
- Subudhi AK**, Green JL, Satyam R, Lenz T, Salunke RP, Shuaib M, Isaioglou I, Abel S, Gupta M, Esau L, Mourier T, Nugmanova R, Mfarrej S, Sivapurkar R, Stead Z, Rached FB, Otswal Y, Sougrat R, Dada A, Kadamany AF, et al. 2023. PfAP2-MRP DNA-Binding Protein Is a Master Regulator of Parasite Pathogenesis during Malaria Parasite Blood Stages. *bioRxiv*. DOI: <https://doi.org/10.1101/2023.05.23.541898>
- Toenhake CG**, Fraschka SAK, Vijayabaskar MS, Westhead DR, van Heeringen SJ, Bártfai R. 2018. Chromatin Accessibility-based characterization of the gene regulatory network underlying *Plasmodium falciparum* blood-stage Development. *Cell Host & Microbe* **23**:557–569. DOI: <https://doi.org/10.1016/j.chom.2018.03.007>, PMID: 29649445
- Trager W**, Jensen JB. 1976. Human malaria parasites in continuous culture. *Science* **193**:673–675. DOI: <https://doi.org/10.1126/science.781840>, PMID: 781840
- Wagner EJ**, Carpenter PB. 2012. Understanding the language of Lys36 methylation at histone H3. *Nature Reviews. Molecular Cell Biology* **13**:115–126. DOI: <https://doi.org/10.1038/nrm3274>, PMID: 22266761
- Ward P**, Equinet L, Packer J, Doerig C. 2004. Protein kinases of the human malaria parasite *Plasmodium falciparum*: the kinome of a divergent eukaryote. *BMC Genomics* **5**:79. DOI: <https://doi.org/10.1186/1471-2164-5-79>, PMID: 15479470
- Yeoh S**, O'Donnell RA, Koussis K, Dluzewski AR, Ansell KH, Osborne SA, Hackett F, Withers-Martinez C, Mitchell GH, Bannister LH, Bryans JS, Kettleborough CA, Blackman MJ. 2007. Subcellular discharge of a serine protease mediates release of invasive malaria parasites from host erythrocytes. *Cell* **131**:1072–1083. DOI: <https://doi.org/10.1016/j.cell.2007.10.049>, PMID: 18083098
- Yuda M**, Iwanaga S, Shigenobu S, Mair GR, Janse CJ, Waters AP, Kato T, Kaneko I. 2009. Identification of a transcription factor in the mosquito-invasive stage of malaria parasites. *Molecular Microbiology* **71**:1402–1414. DOI: <https://doi.org/10.1111/j.1365-2958.2009.06609.x>, PMID: 19220746
- Yuda M**, Kaneko I, Murata Y, Iwanaga S, Nishi T. 2023. Targetome Analysis of Malaria Sporozoite Transcription Factor AP2-Sp Reveals Its Role as a Master Regulator. *mBio* **14**:e0251622. DOI: <https://doi.org/10.1128/mbio.02516-22>, PMID: 36622145
- Zhang M**, Wang C, Otto TD, Oberstaller J, Liao X, Adapa SR, Udenze K, Bronner IF, Casandra D, Mayho M, Brown J, Li S, Swanson J, Rayner JC, Jiang RHY, Adams JH. 2018. Uncovering the essential genes of the human malaria parasite *Plasmodium falciparum* by saturation mutagenesis. *Science* **360**:eaap7847. DOI: <https://doi.org/10.1126/science.aap7847>, PMID: 29724925
- Zhang Y**, Bertulat B, Tencer AH, Ren X, Wright GM, Black J, Cardoso MC, Kutateladze TG. 2019. MORC3 Forms Nuclear Condensates through Phase Separation. *iScience* **17**:182–189. DOI: <https://doi.org/10.1016/j.isci.2019.06.030>, PMID: 31284181
- Zhong Z**, Xue Y, Harris CJ, Wang M, Li Z, Ke Y, Liu M, Zhou J, Jami-Alahmadi Y, Feng S, Wohlschlegel JA, Jacobsen SE. 2023. MORC proteins regulate transcription factor binding by mediating chromatin compaction in active chromatin regions. *Genome Biology* **24**:96. DOI: <https://doi.org/10.1186/s13059-023-02939-4>, PMID: 37101218